

# Meteor Berichte 03-04

## *Mid-Atlantic Expedition 2004*

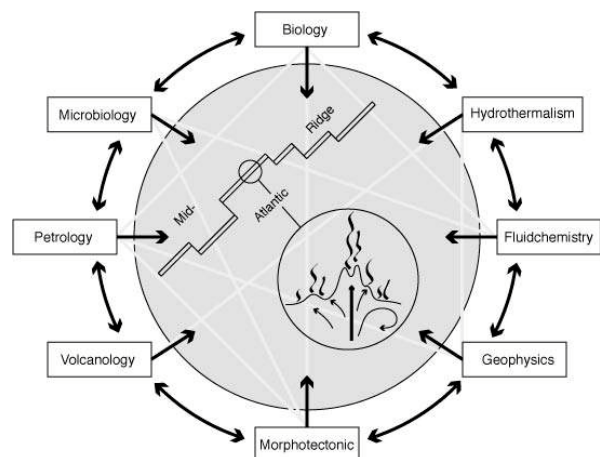
### Cruise No. 60, Leg 3

Mineralogical, geochemical, and biological investigations of hydrothermal systems on the Mid-Atlantic Ridge between 14°45'N and 15°05'N (HYDROMAR I)

14 January – 14 February 2004, Fort-de-France – Fort-de-France (Martinique)

T. Kuhn, B. Alexander, N. Augustin, D. Birgel, C. Borowski, L.M. de Carvalho, G. Engemann, S. Ertl, L. Franz, C. Grech, R. Hekinian, J.F. Imhoff, T. Jellinek, S. Klar, A. Koschinsky, J. Kuever, F. Kulescha, K. Lackschewitz, S. Petersen, V. Ratmeyer, J. Renken, G. Ruhland, J. Scholten, K. Schreiber, R. Seifert, J. Süling, M. Türkay, U. Westernströer, F. Zielinski

Project Leader: Peter M. Herzig



Leitstelle Meteor  
Institut für Meereskunde der Universität Hamburg



## Summary

The *R/V METEOR* cruise M60/3 took place from January 13 through February 14, 2004 from/to Fort-de-France (Martinique) and led to the Logatchev hydrothermal fields situated on the Mid-Atlantic Ridge (MAR) at 14°45'N and 44°59'W as well as to a working area II at 14°55'N and 44°55'W. The main mapping and sampling tool used during the cruise was the ROV (Remotely Operated Vehicle) QUEST provided by the University of Bremen.

The active Logatchev hydrothermal field lies on a small plateau on the eastern flank of the inner rift valley in 2900 m to 3060 m water depth. It is characterized by sites of active, high-T fluid emanation and sulfide precipitation as well as by inactive sites. Extensive bathymetric and video mapping during the M60/3 cruise revealed three factors which appear to control the location of the Logatchev hydrothermal field: (1) cross-cutting faults, (2) young basaltic volcanism, and (3) slump structures forming probably thick talus deposits. Furthermore a new, but inactive hydrothermal field (Logatchev-4 at 14°42.38'N / 44°54.50'W) was discovered during M60/3. Our investigations show that hydrothermal circulation may have taken place through talus material and has altered peridotite debris. The heat is probably supplied from magmatic bodies associated with basaltic melts localized underneath the adjacent rift valley and/or off-axis volcanic structures. Heat could also be provided by localized intrusion of melts (probably focussed along faults) into the peridotite. To date, a situation similar to that of the Logatchev area has only been found at 14°54'N / 44°55'W (Eberhardt et al., 1988). The similarity of the local geological setting to that of the Logatchev area indicates that this region has hydrothermal potential.

Mapping and sampling with ROV QUEST and the TV-grab revealed that the active Logatchev-1 hydrothermal field is larger than previously described. It extends at least 800 m in a NW-SE and probably more than 400 m in a SW-NE direction. Two main areas of high-temperature (high-T) hydrothermal activity make up the central part of the field: an area of at least three „smoking craters“ (ANNA-LOUISE, IRINA and SITE „B“) and the large mound of IRINA II with black smoker chimneys at its top as well as the newly discovered QUEST smoking crater. The smoking craters consist of a rampart-like rim that is 1-2 m high and a 2-3 m deep central depression. Dense mussel beds were absent in these environments, macrofauna was generally sparse. However, abundant microbial mats were seen at locations where the black smoke emanating from the sea floor passes over rock surfaces. IRINA II consists of a mound (basal diameter of about 60 m) with steep slopes rising about 15 m above the surrounding seafloor. Four vertical chimneys, a couple of meters high, mark the top of the mound. In contrast to the smoking craters they are densely overgrown with and surrounded by mussels. QUEST is a newly discovered high-T, black smoke venting site situated about 130 m WNW (in 330° direction) of the active chimneys of IRINA II.

Hydrothermal fluids (both high- and low-T) display similar patterns of their chemical composition suggesting the presence of a single fluid type. The emanating high-T fluids are strongly reducing have high methane and hydrogen contents and low sulfide concentrations. Iron is the dominant dissolved and particle-bound metal. However, all hydrothermal fluid samples were diluted by seawater and the results presented here are not yet recalculated to endmember compositions. Methane and hydrogen but also metal sulfides are considered to be the major energy sources for the development of life in the Logatchev field.

Host rocks of the Logatchev field sampled by TV-grab and ROV were mainly serpentinized peridotites while basalts and gabbros (sometimes in magmatic contact with peridotite) occurred subordinately. Remarkable were samples of coarse-grained websterites, orthopyroxenites and orthopyroxene-rich, pegmatoidal norites, which were interpreted as magmatic cumulates from the crust/mantle transition zone. A large variety of hydrothermal precipitates was recovered including chalcopyrite chimneys, massive pyrite crusts, silicified breccias, abundant secondary Cu-sulfides (including native copper), red jaspers, abundant Fe-Mn-oxyhydroxides as well as atacamite and Mn-oxides. The occurrence of massive sulfides as crusts overlying altered host rock material along the flanks of the deposit suggests that they might only be a thin veneer directly at or below the seafloor.

We are grateful to captain M. Kull, the officers and the crew of the R/V METEOR as well the ROV crew for their excellent performance and co-operation which was primordial for the success of the cruise. We are also thankful to G. Cherkashov for providing Russian data and maps prior to the HYDROMAR cruise. The German Research Foundation (DFG) funded this cruise which was carried out within the framework of the DFG Priority Program 1144: From Mantle to Ocean: Energy-, Material- and Life-cycles at Spreading Axes.

### 3.1 Participants

	Name	Discipline	Institution
1.	Kuhn, Thomas, Dr. / Chief Scientist	Geochemistry	TUBAF/ IfM-GEOMAR
2.	Alexander, Brian	Fluid Chemistry	IUB
3.	Augustin, Nico	Petrology	GeoB
4.	Birgel, Daniel	Biogeochemistry	RCOM
5.	Borowski, Christian, Dr.	Microbiology	MPI-Bremen
6.	de Carvalho, L.M., Dr.	Fluid Chemistry	UFSM
7.	Engemann, Greg	ROV	ASR
8.	Ertl, Siegmund, Dr.	Gas Chemistry	IfBM
9.	Franz, Leander, PD Dr.	Petrology	TUBAF
10.	Grech, Chris	ROV	MBARI
11.	Hekinian, Roger Dr.	Geochemistry	IGW
12.	Imhoff, Johannes, Prof. Dr.	Microbiology	IfM-GEOMAR
13.	Jellinek, Thomas, Dr.	Zoology	Senckenberg
14.	Koschinsky-Fritsche, Andrea, PD Dr.	Fluid Chemistry	IUB
15.	Klar, Steffen	ROV	GeoB/MARUM
16.	Küver, Jan, Dr.	Microbiology	MPA
17.	Kulescha, Friedhelm	Technician	Oktopus
18.	Lackschewitz, Klas, Dr.	Petrology	GeoB
19.	Petersen, Sven, Dr.	Geochemistry	TUBAF
20.	Ratmeyer, Volker, Dr.	ROV	MARUM
21.	Renken, Jens	ROV	MARUM
22.	Ruhland, Götz	ROV	MARUM
23.	Scholten, Jan, Dr.	Geochemistry	IGW
24.	Schreiber, Kerstin	Geochemistry	TUBAF
25.	Seifert, Richard, Dr.	Gas Chemistry	IfBM
26.	Süling, Jörg, Dr.	Microbiology	IfM-GEOMAR
27.	Truscheit, Torsten	Meteorology	DWD
28.	Türkay, Michael, Dr.	Zoology	Senckenberg
29.	Westernströer, Ulrike	Fluid Chemistry	IGW
30.	Zielinski, Frank	Microbiology	MPI-Bremen

ASR Alstom Schilling Robotics

201 Cousteau Place

Davis, CA 95616 / USA

DWD

Deutscher Wetterdienst

Geschäftsfeld Seeschifffahrt

Bernhardt Nocht Str. 76

20359 Hamburg / Germany

GeoB

Universität Bremen

FB Geowissenschaften

Postfach 330440

28334 Bremen / Germany

---

IfBM	Universität Hamburg Institut für Biogeochemie und Meereschemie Bundesstr. 55 D-20146 Hamburg / Germany
IfM-GEOMAR	Leibniz-Institut für Meereswissenschaften Düsternbrooker Weg 20 D-24105 Kiel / Germany Wischhofstr. 1-3 D-24148 Kiel / Germany
IGW	Universität Kiel Institut für Geowissenschaften Olshausenstr. 40 D-24098 Kiel / Germany
IUB	International University Bremen Geosciences and Astrophysics P.O. Box 750561 D-28725 Bremen / Germany
MARUM	Zentrum für Marine Umweltwissenschaften Universität Bremen Klagenfurter Str. D-28359 Bremen / Germany
MBARI	Monterey Bay Aquarium Research Institute 7700 Sandthold Road Moss Landing, CA 95039-9644 / USA
MPA	Amtliche Materialprüfungsanstalt Bremen Paul Feller Str. 1 28199 Bremen / Germany
MPI-Bremen	Max-Planck-Institut für Marine Mikrobiologie Celsiusstr. 1 D-28359 Bremen / Germany
Oktopus GmbH	Kieler Str. 51 D-24594 Hohenwestedt / Germany
RCOM	Forschungszentrum Ozeanränder an der Universität Bremen Postfach 330440 D-28334 Bremen / Germany
Senckenberg	Forschungsinstitut Senckenberg Senckenberganlage 25 D-60325 Frankfurt a. M. / Germany
TUBAF	TU Bergakademie Freiberg Institut für Mineralogie Lehrstuhl für Lagerstättenlehre und Leibniz-Labor für Angewandte Meeresforschung Brennhausgasse 14 D-09596 Freiberg / Germany
UFSM	Universidade Federal de Santa Maria Caixa Postal 5051 97110-970 Santa Maria-RS / Brasil

### 3.2 Research Program

(Thomas Kuhn)

The principal scientific aim of **leg M60/3** was to investigate the relationship of geological and biological processes in active, ultramafic-hosted hydrothermal systems on the Mid-Atlantic Ridge (MAR) between 14°45'N and 15°05'N. Two different sample locations were targeted: (i) the active Logatchev hydrothermal field at 14°45'N which hosts massive sulfides and (ii) the area at 14°55'N where a hydrothermal field was described from photo sled investigations and where outcropping oceanic mantle rocks were sampled during previous cruises. The main tools for seafloor investigations and sampling were the new 4000m workclass ROV QUEST provided by the University of Bremen (c/o Prof. G. Wefer, Dr. V. Ratmeyer, MARUM) and the TV-grab. Special tools were adapted to the ROV for biological and fluid sampling.

The research objectives focused on the chemistry of hydrothermal fluids and minerals in relation to the tectonic activity, the composition of the oceanic lithosphere, and the activity of hydrothermal biota. An important question is, whether there is a genetic link between the hydrothermally active Logatchev field and the ultramafic rocks which host the hydrothermal precipitates. The results of these investigations will also improve our understanding of the formation processes of massive sulfide deposits on land which are hosted by ultramafic rocks. Geochemical and biological work focused on the interaction of hydrothermal fluids and biota in hydrothermal systems. Major objectives are the analyses of chemical species in the hydrothermal fluids (both, gaseous species and metals) and their interaction with the colonization patterns, the functional roles and the activity patterns of hydrothermal bacteria, archaea and fauna. A central issue in these investigations is the transition of inorganic and organic compounds and energy that is provided by electron donating reduced gases (i.e. diluted H<sub>2</sub>, H<sub>2</sub>S, CH<sub>4</sub>) from the geochemical level to the biological level of the hydrothermal communities. The influence of supercritical phase separation on the fluid chemistry, mineral precipitation and the structure of hydrothermal communities are also addressed.

Hydrothermal systems hosted by ultramafic rocks, which are characterized by active hydrothermalism as well as active serpentinization, are especially suitable for combined research on the above-mentioned scientific objectives. The research cruise M60/3 was carried out within the frame of the DFG-Priority Program 1144 "From Mantle to Ocean: Energy-, Material- and Life-cycles at Spreading Axes".

### 3.3 Narrative of the Cruise

(Thomas Kuhn)

Cruise M60/3 started on January 13, 2004 in Fort-de-France (Martinique) with loading the scientific equipment onboard R/V METEOR, the built-up of the ROV QUEST as well as a harbour test of a new deployment frame for the ROV. The scheduled departure on January 15 had to be postponed for 33 hours due to a faulty acoustic array of the POSIDONIA navigation system. Since the exact positioning of the ROV was an essential part of the scientific work, we decided to wait for a spare one which was sent from France. On January 16, at 21:20 LT

R/V METEOR departed from Fort-de-France and started its transit to the Logatchev hydrothermal field at 14°45'N and 44°59'W.

The working area was reached on January 20 at 20:00 LT. Scientific work started with the deployment of a reference station for the POSIDONIA ROV navigation. During the night HYDROSWEEP mapping, a CTD station as well as the calibration of the reference station kept the vessel busy.

Due to two crossing swells which caused strong rolling vessel movements the first ROV station could not be carried out on January 21. Instead, the HYDROSWEEP mapping was continued. During the night a long TV-sled (st. 22, Fig. 3.1) track was run over the eastern rift valley flank crossing the Logatchev-1 hydrothermal field down to the central valley floor. Since the weather and sea conditions improved on January 22 the first ROV station could be carried out. The swell still was about 2-3 m and both the ROV and the ship's crew made a very good job to deploy the ROV QUEST. In the course of this first ROV station the northwestern part of the Logatchev-1 hydrothermal field was mapped and sampled in 3060 m to 3050 m water depth. A previously unknown site with diffuse venting hydrothermal fluids, a mussel field and wide-spread bacterial mats were discovered south of ANYA'S GARDEN. A temperature logger was deployed and fluid measurements carried out. After the investigation of this diffuse venting site, QUEST moved to the IRINA II complex about 100 m ESE (Fig. 3.2). This complex consists of a mound structure of about 60 m diameter at its base and 15 m height. Active black smoker chimneys, 2-4 m high, are situated on its top. The chimneys are densely overgrown by hydrothermal fauna and are surrounded by mussel fields. A temperature logger and a homer beacon were placed close to a marker of the French-Russian campaign MICROSMOKE. All ROV systems worked well and the video data were of excellent quality.

HYDROSWEEP mapping was carried out during the night. On January 23 a first TV-grab station in the Logatchev-1 field was unseccussful due to a technical failure of the grab. The following TV-sled transect (st. 27) from the rift mountains at 1600 m water depth to the so-called Logatchev-2 field in 2650 m water depth discovered a new hydrothermal field. Since three hydrothermal fields called Logatchev-1 to Logatchev-3 were previously known in this area, we called the new one Logatchev-4 (Fig. 3.1). It is an inactive field with beds of empty shells and is about 90 m long. It was found about 50 m below a ENE-WSW ridge. It seems that the shells were displaced from the ridge. The exact position of the TV-sled on the seafloor was calculated using the POSIDONIA system (with a transponder mounted on the sled). HYDROSWEEP mapping was continued during the night.

During station 29ROV on January 24 the area between IRINA II and IRINA was mapped (Fig. 3.2). Two so-called smoking craters (site "B" and IRINA) were investigated and fluid samples were taken. Due to a drop of oil pressure the station had to be aborted and no sulfide samples could be taken. HYDROSWEEP mapping was continued during the night.

Three TV-grab stations were carried out on January 25 (32, 33, 35GTV; Fig. 3.2). Numerous samples of massive sulfides and crusts, vein quartz, mussel beds on silicified hydrothermal crusts, atacamite as well as ultramafic rocks with different degrees of serpentinization were sampled. Two hydrocast profiles were carried out north of and within the Logatchev-1 field.

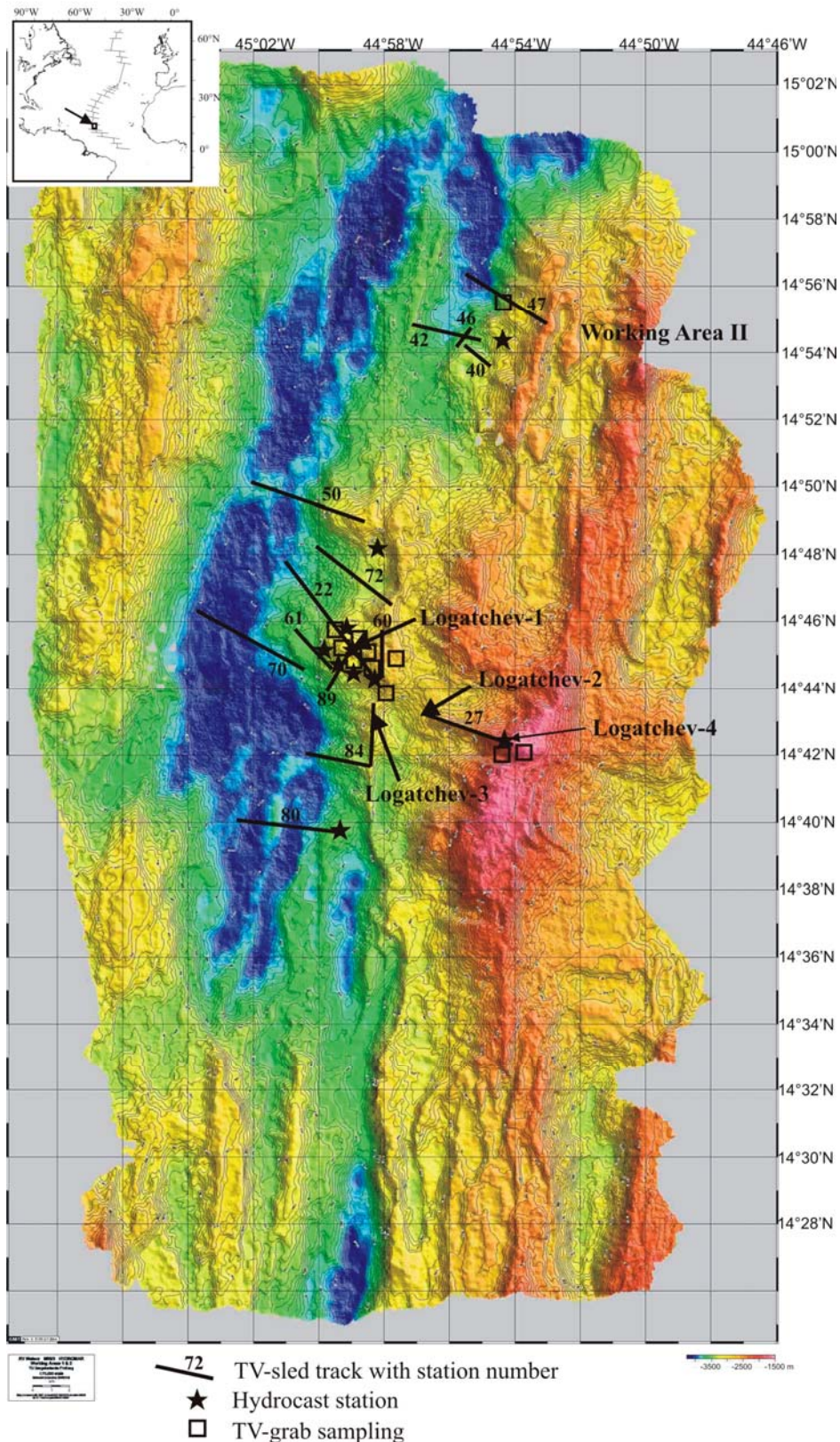


**Fig. 3.1:** Bathymetric map of the working area produced with HYDROSWEEP during M60/3. TV-sled, hydrocast (CTD/Ro.) and TV-grab sampling stations are also shown. All ROV operations were carried out in the Logatchev-1 hydrothermal field. Insert: Location of the working area on the MAR

On January 26 station 38ROV was reserved for biological and fluid-chemical work at the IRINA II complex. At the beginning of the station two baited traps were deployed on the mussel beds near the chimney complex. They were recovered at the end of the station. Diffusely venting fluids were sampled for geochemical and microbiological investigations, hydrothermal fauna was collected for taxonomic and molecular research. Detailed video images of the habitat of shrimps and mussels were recorded. The total duration of the station (from deck to deck) was 14 hours. It started with technical checks at 8:00 a.m. which took about 1 hour, lowering and heaving through the water column took 4 hours in total, therefore time for the work at the seafloor was 8-9 hours.

The Russian R/V PROFESSOR LOGATCHEV arrived at the working area on the evening of January 26. Captain (M. Kull), the chief scientist (T. Kuhn) and two other scientists (K. Lackschewitz and R. Hekinian) went over to the Russian vessel to discuss and organize the research work of the coming days. After a two hours visit they returned to the R/V METEOR.

A two hours transit to working area II at 14°55'N and 44°55'W was followed by two TV-sled tracks (st. 40, 42; Fig. 3.1) interrupted by HYDROSWEEP mapping on January 27. The objective of these tracks was to map the area and to relocate a hydrothermal field which was suggested by other workers (Eberhardt et al., 1988). Rather young basalts, small pillow mounds and ridges, some larger scarps and crosscutting faults were observed, but no hydrothermal activity was found. Unfortunately two attempts of ROV deployment failed due to bad sea conditions and a winch problem. A hydrocast station (st. 44 on January 28) close to a station of Charlou et al. (1993) detected strong methane and hydrogen anomalies in the water column at least suggesting strong serpentinization in this area (Fig. 3.1). Two more TV-sled tracks (st. 46, 47; Fig. 3.1) on January 29 were conducted to map the contact between ultramafics and basalts in working area II above the suggested hydrothermal field. According to the results of station 47 a TV-grab taken right beneath a scarp sampled ultramafic rocks which, in one case, showed mylonitic textures, in another a magmatic contact between ultramafics and basalts (see Chapter 3.4.6). HYDROSWEEP mapping carried out on January 28 and 29 filled gaps in the bathymetric map. Another TV-sled station (st. 50) carried out along the eastern flank of the rift valley between working area I and II revealed only ultramafic rocks even in the rift valley. The rift axis area consists of a succession of undulating hills. Three fissures most likely mark the current rift axis.

During the night between January 29 and 30, R/V METEOR returned to working area I (Logatchev fields). Two hydrocast stations south of the Logatchev-1 hydrothermal field investigated the hydrothermal plume dispersal in the water column. On January 30 sea conditions made the next ROV station (53ROV) possible. This geological dive aimed at detailed mapping and sampling of the smoking craters IRINA and ANNA-LOUISE (Fig. 3.2). The general dimension and structure of the smoking craters was mapped and video-recorded, active and inactive chimneys were sampled using both manipulators. Fluid samples from black smokers on the rim of the smoking craters were also taken. Another TV-grab (54GTV) was taken on a small mound about 100 m to the east of the smoking crater area in order to sample the periphery of the Logatchev-1 field (Fig. 3.2). The samples consist of secondary Cu-sulfides with carbonate veins, silica and grains of native copper suggesting that this area also was a site of high-temperature precipitation in the past which is now in a state of oxidation. During the night HYDROSWEEP mapping was continued.

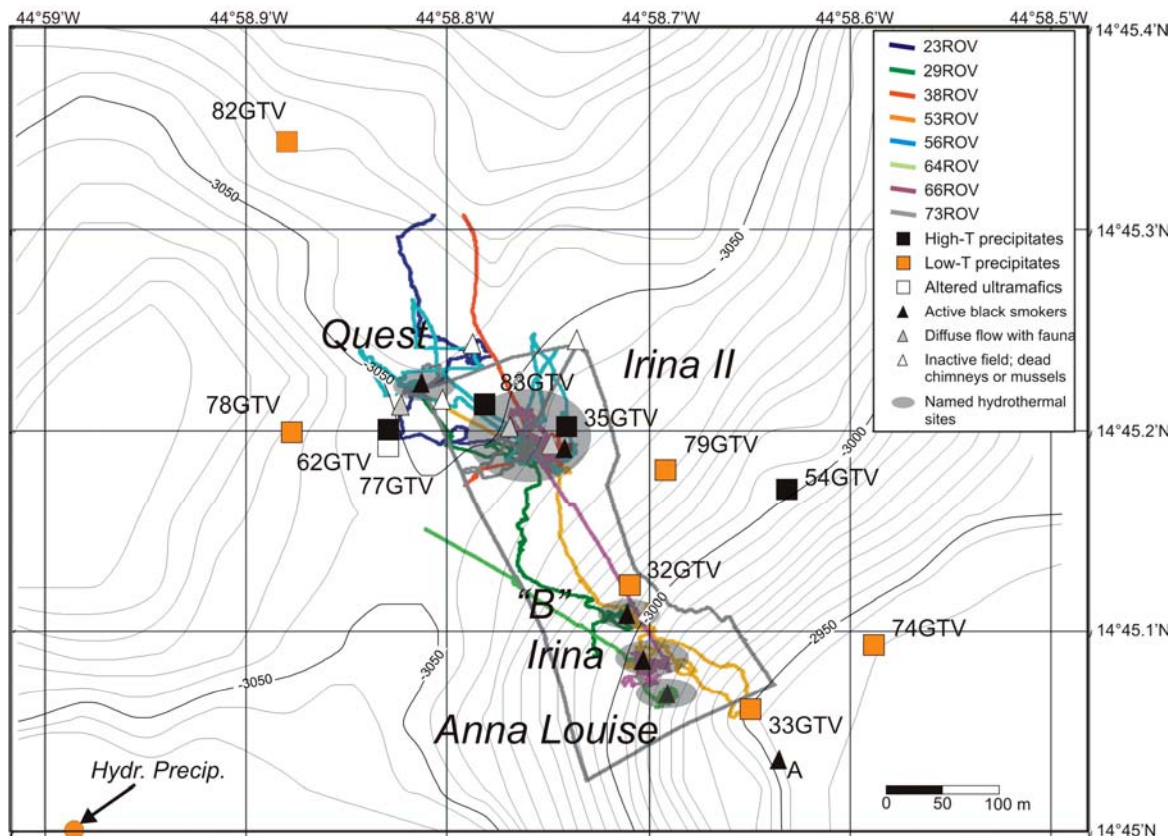


**Fig. 3.2:** Logatchev-1 hydrothermal field with ROV tracks and TV-grab stations carried out during M60/3. QUEST is a newly discovered site venting high-temperature black smoke. Site "A" was not observed during M60/3 but described in literature (Gebruk et al., 2000). Hydrothermal precipitates (but no current hydrothermal activity) were also observed during station 89OFOS about 500 m to the SW of the Logatchev-1 field.

During dive 56ROV on January 31 biological and fluid samples were taken from IRINA II and ANYA'S GARDEN (Fig. 3.2). A special objective was the investigation of ANYA'S GARDEN since this site was described as a place where species of *Calyptogena* should occur. This species is specialized in  $H_2S$ -rich fluids and therefore this site should be different from other sites of the Logatchev-1 field where  $CH_4$ - and  $H_2$ -rich fluids emanate. However, no field with *live Calyptogena* could be found, neither at the location of the marker ANYA (this marker was not in the place where it should be according to literature; Gebruk et al., 2000) nor at the location described by other authors. However, during dive 56ROV a new black smoker venting site was detected and named after the ROV as QUEST site (Fig. 3.2). At this site but also at the smoker complex of IRINA II samples of *Bathymodyolus* and *Calyptogena* (a few specimen of *Calyptogena* occurred) together with shrimps (*Rimicaris exoculata*) and accompanying fauna (crabs, polychaets etc.) were taken. At QUEST bacterial mats were sampled with a special shovel adapted to the ROV. Directly above the mats fluid samples were also taken and fluid parameters (T,  $O_2$ , Redox,  $H_2S$ ) were measured with an in-situ fluid measuring system (PROFILUR). Station 56ROV ended at 21:00 on January 31. The following night and during February 1 a TV-grab station on the shallowest point of the eastern valley walls (1600 m water depth; Fig. 3.1) and two hydrocast stations to the west and southwest of

the Logatchev-1 field were carried out. The TV-grab sampled different types of serpentinized ultramafic rocks, basalts and one amphibolite. The hydrocast revealed several methane and hydrogen anomalies in different water depths. Later this day two TV-sled tracks (st. 60, 61; Fig. 3.1) were run in the areas east and west of Logatchev-1. The objective of st. 60 was to map the plateau above the Logatchev-1 field and of st. 61 to map the contact between ultramafics and basalts and to investigate the round-shaped feature close to the central valley floor (Fig. 3.1).

The night to February 2 was filled with another TV-grab station (62GTV) to sample an area west of the main active zone of the Logatchev-1 field. This grab sampled serpentinized and mineralized ultramafics, pyroxenites, scoriaceous black breccia and also sulfide-rich material. After two HYDROSWEEP profiles, the next ROV QUEST station (64ROV) was aimed at mapping and sampling the smoking crater ANNA LOUISE for geological and geochemical investigations (Fig. 3.2). Apart from this work, temperature loggers were recovered from IRINA which measured diffusely venting hydrothermal fluids for 3.5 days. February 2 was completed by HYDROSWEEP profiles.

QUEST station 66ROV on February 3 again concentrated on biological and fluid-chemical sampling and experiments at sites IRINA and IRINA II. Microbial mats were sampled at locations where black smoke emanating from the sea floor was in contact with rock surfaces close to an old marker at IRINA (FIG. 3.2). Temperature measurements were carried out and fluid samples taken immediately above these bacterial mats. At the northwestern slope of the IRINA II mound only empty shells of *Calyptogena* but living ones of *Bathymodiolus* were found. At this site of diffuse venting living mussels were sampled. The sampling was completed by fluid samples and measurements of fluid parameters with PROFILUR.

On February 4 one TV-grab station (67GTV), three hydrocast stations and one TV-sled track (st. 70) were carried out. The TV-grab was aimed at sampling the Logatchev-4 hydrothermal field (Fig. 3.1). However, due to the very steep morphology it was only possible to take samples about 50 m below the field. The samples consisted of coarse-grained pyroxenites, peridotites and metabasalts in direct contact with ultramafics and one empty shell of *Bathymodiolus*. The hydrocast stations were carried out in the N, S, and E of Logatchev-1. A transponder was mounted on the hydrocast frame for exact positioning using the POSIDONIA system. The objective of these stations was to investigate the hydrothermal plume structure of the Logatchev-1 field. Mapping of the central valley floor close to the Logatchev-1 field was the objective of the TV-sled station.

February 5 started with another TV-sled (st. 72) which investigated steep morphological structures at the eastern rift flank north of the Logatchev-1 field and mapped the contact between ultramafics and basalt. It turned out that the seafloor consists of several nearly vertical escarpments which may mark young fault zones along which mantle material was tectonically emplaced. After this TV-sled track another ROV station (73ROV) explored the immediate surroundings of the Logatchev-1 field in order to map possible fault planes, to map the arial extension of the currently hydrothermally active area and to add information about how far hydrothermal precipitates reach away from the current active zone (Fig. 3.2). It could be shown during this station that the Logatchev-1 field extends far more to the N and SW than previously known. Some samples from inactive chimneys at IRINA II were also sampled

using the manipulators of the ROV and two baited traps were deployed at a mussel field close to the smoker complex of IRINA II. Station 73ROV was followed by another TV-grab (74GTV) which sampled the mound that was mapped east of the smoking craters during the previous ROV station.

February 6 was used for hydrocast, TV-grab and TV-sled stations. A ROV deployment was not possible due to increasing and crossing swells from E and NNW. The hydrocast stations (75, 76 CTD/Ro) sampled the hydrothermal plumes to the SSW of the Logatchev-1 field. Three TV-grab stations (st. 77, 78, 79; Fig. 3.2) were aimed at sampling the periphery to the E and W of the Logatchev-1 field and also to get rock samples from the surrounding of the field. All three stations were successful and recovered low-T hydrothermal precipitates which mark the distal part of the hydrothermal field where strong dilution of hydrothermal fluids by entraining seawater prevails. During the TV-sled track of st. 80 an area about 5 nm to the south of the Logatchev-1 field was mapped where a distinct methane anomaly (but only a weak hydrogen anomaly) was found in 2800 m water depth (Fig. 3.1). The track started at the eastern flank of the rift valley, crossed the position of the methane anomaly and was continued over most parts of the central valley mapping a pillow basalt ridge.

The wind continuously increased to Bft. 8 on February 7 and the sea swell also gradually built up. Therefore, a ROV station was still impossible on this day. We continued our geological and geochemical program with two hydrocasts in the area SE of Logatchev-1, one TV-grab and one TV-sled station. The hydrocast stations should further improve our understanding of the hydrothermal plume structure around Logatchev-1. Station 83GTV (Fig. 3.2) aimed at sampling a mussel bed for a statistical analysis of the size distribution of species *Bathymodiolus*. The TV-sled track (st. 84) was run over Logatchev-3 to map the hydrothermal precipitates and the distribution of ultramafics and basalts in this area (Fig. 3.1).

The bad weather with heavy sea and wind continued on February 8 and therefore no ROV deployment was possible. Instead, the geological and geochemical program was continued as on February 7 with two hydrocast stations, one directly over Logatchev-1 and one to the SSW, one TV-grab and one TV-sled. The objective of the TV-grab (st. 87) was to sample large-sized ultramafic rock samples close to Logatchev-1 for separating zircon for age dating. The TV-sled track (st. 89) was carried out from the Logatchev-1 field to the SSW in order to map fault structures and the contact between ultramafics and basalt. During this station hydrothermal precipitates were discovered about 600 m WSW of ANNA LOUISE (Fig. 3.2). If there is a connection between Logatchev-1 and these precipitates, this hydrothermal field would be much larger than previously known. The recovery of the reference station was also realized on February 8.

The station work was finished on February 9 at 03:35 LT and R/V METEOR started its transit to Fort-de-France. Arrival in FdF was on February 13 at 08:00 LT. Containers were unloaded from the vessel on this day and the cruise M60/3 ended on February 14 with the disembarkation of the scientific crew.

The original scientific program included a third working area at 15°05'N/44°58'W (20 nm north of the Logatchev field) to be investigated with the ROV QUEST. However, the main working area was the Logatchev-1 hydrothermal field. Especially, the biological and fluid chemistry groups concentrated on this working area. They needed a minimum number of 10

ROV stations for their experiments and sampling. Since we could carry out only 9 successful ROV stations in the entire Logatchev field we had to stay there in order to get another chance if the weather increased. However, the bad weather conditions also stayed during the last days of the cruise and made another ROV deployment impossible. Therefore, we decided to do more geological (TV-sled and –grab) and water-chemical work (hydrocast) in the Logatchev field for a better understanding of this area instead of going to working area III where gathering new knowledge on top of what was already known would have been impossible without the ROV.

### **3.4 Preliminary Results**

#### **3.4.1 Seafloor mapping and structural geology**

(R. Hekinian, T. Kuhn)

##### **3.4.1.1 Introduction**

In contrast to the fast spreading East Pacific Rise (EPR), the Mid-Atlantic Ridge (MAR) with its low spreading rates ( $< 3$  cm/yr, total rate) consist of ridge segments with a more discontinuous and irregular shaped structure. These ridge segments away from the influence of large mantle plume upwelling zone such the Azores and Iceland show also thinner crust gashed by a deep ( $>3000$ m) central rift valley. Thin crust suggests a low rate of magmatism and the eventual exposure of lower and upper mantle material, such as ultramafics and gabbro. Thus magma-starved segments of the MAR are found in the equatorial region between  $12^{\circ}\text{N}$  and  $16^{\circ}\text{N}$ . These areas are also characterized by short ridge segments interrupted by non-transform discontinuities as well as closely spaced major fracture zones such as those located between  $5^{\circ}\text{N}$  and  $5^{\circ}\text{S}$  which extend from African to Brazilian coasts.

In 1993-1994 the Russian scientific team aboard the R/V PROFESSOR LOGATCHEV has found a hydrothermal field which they called the “Logatchev field” located on the eastern rift mountain of the MAR south of the “Fifteen-Twenty fracture zone and near  $14^{\circ}45'\text{N}$  (Batuyev et al., 1994). The main characteristic of the spreading ridge segment at  $14^{\circ}45'\text{N}$  is the presence of important serpentinized peridotite outcropping on the rift valley floor as well as on the eastern and western walls of the ridge axis.

Also, during previous exploration along the MAR it was found that the rift valley flanks are sometimes the main location for hydrothermalism associated with ultramafics as well as with MORB. This was observed for example at  $26^{\circ}00'\text{N}$ - $26^{\circ}13'\text{N}$  in the TAG and at  $14^{\circ}$ - $15^{\circ}\text{N}$  on step faulted terrains of the rift valley eastern marginal walls (Batuyev et al., 1994; Rona et al., 1992). Although most hydrothermal sites are associated with basaltic lavas erupted in the axial valley, two areas of the MAR which were studied in detail are known to have been the sites of hydrothermal activities forming sulfide deposits on top of ultramafic rocks. These areas are the Rainbow hydrothermal field near  $36^{\circ}14'\text{N}/33^{\circ}54.12'\text{W}$  (German et al., 1998) and the Logatchev fields near  $14^{\circ}45'\text{N}$ - $45^{\circ}00'\text{W}$  (Batuyev et al., 1994).

The origin of these hydrothermal deposits constructed on top of ultramafics is not well assessed and controversial. Are these hydrothermal deposits directly connected with the leaching of ultramafic complexes of lower crust-upper mantle composition? Or are they, instead, related to the leaching of the mafic components (basalt-dolerite-gabbro) intruded into

the lithosphere? If the hydrothermal precipitates originated from the basaltic and/or mafic intrusive dolerite than it is likely that hydrothermal circulation would take place within basaltic basement formed at the ridge axis. Another alternative to this hypothesis is that the off-axis hydrothermal venting and the associated ultramafics are underlain by basaltic units. This implies that the ultramafic complex on which the hydrothermal deposits are formed represent large mass-wasted material covering the basaltic basement. This is further discussed below.

### **3.4.1.2 Rift valley**

The rift valley floor at 3900-4200 m depth consists of a moderately (< 30%) sedimented area with isolated volcanic constructions forming small mounds and elongated ridges often with step faulted outcrops. The previous sampling of the rift valley, mainly in the northern part (north of 14°50'N), showed the presence of both ultramafics and basaltic rocks. The present study confirms this finding and shows that basaltic outcrops are prominent in the rift valley deeper than 3900 m (Fig. 3.3). It was also found that the spreading is taking place in a narrow zone (< 1 km) with active fault scarps and recent fissures oriented N010°. The younger flows observed are tubular and bulbous lava with preserved small protrusions extruded from the larger pillows. Sheet flows in the form of lobated, flat and ropy surfaces were observed during deep-towed bottom camera stations. The sheet flows often show collapse features of drained lava.

### **3.4.1.3 Rift mountains**

The eastern and the western wall of the rift mountains axis are dissymmetrical with respect to the axis of the MAR spreading center near 14°45'N. In the explored area, the summits of the east and west walls culminate at 1600 meters and 2900 meters, respectively. These contour lines are located at about 10 km and 4 km from the MAR axis. Also the east rift mountain is characterized by several cross-cutting faults. The main orientation of the fault scarps is N010° which also corresponds to the general spreading direction. The other direction of faulting is to N270°-280° which is transverse to the other main fault structures.

The rift mountains region located to the east of the rift valley at 14°45'N and along longitudes 45°00'W and 44°52'W constitutes the prominent features of ridge crest marginal highs oriented to N013° as the MAR axis (Fig. 3.3). The summit of the first discontinuous set of the rift mountain consists of a plateau culminating at about 2900 m water depth that is about 1000 meters above the rift valley floor (4100 m). The eastern wall at the 3050 m contour line shows a narrow, "sliver-like" linear structure oriented to N013° representing the summit of the first rift flank. The top of the rift mountain there is a narrow, "sliver-like" structure (<300 m wide) which has a small east facing depression (<300 m depth). A bottom video camera station (60OFOS) along this plateau near 2970 m depths showed abundant sediment cover and horizontal ledges of ultramafic outcrops associated with patches of inactive hydrothermal fields made up of empty clam shells. This newly discovered field was named Logatchev-4 hydrothermal field according to the already known Logatchev-1 to -3 fields in this area

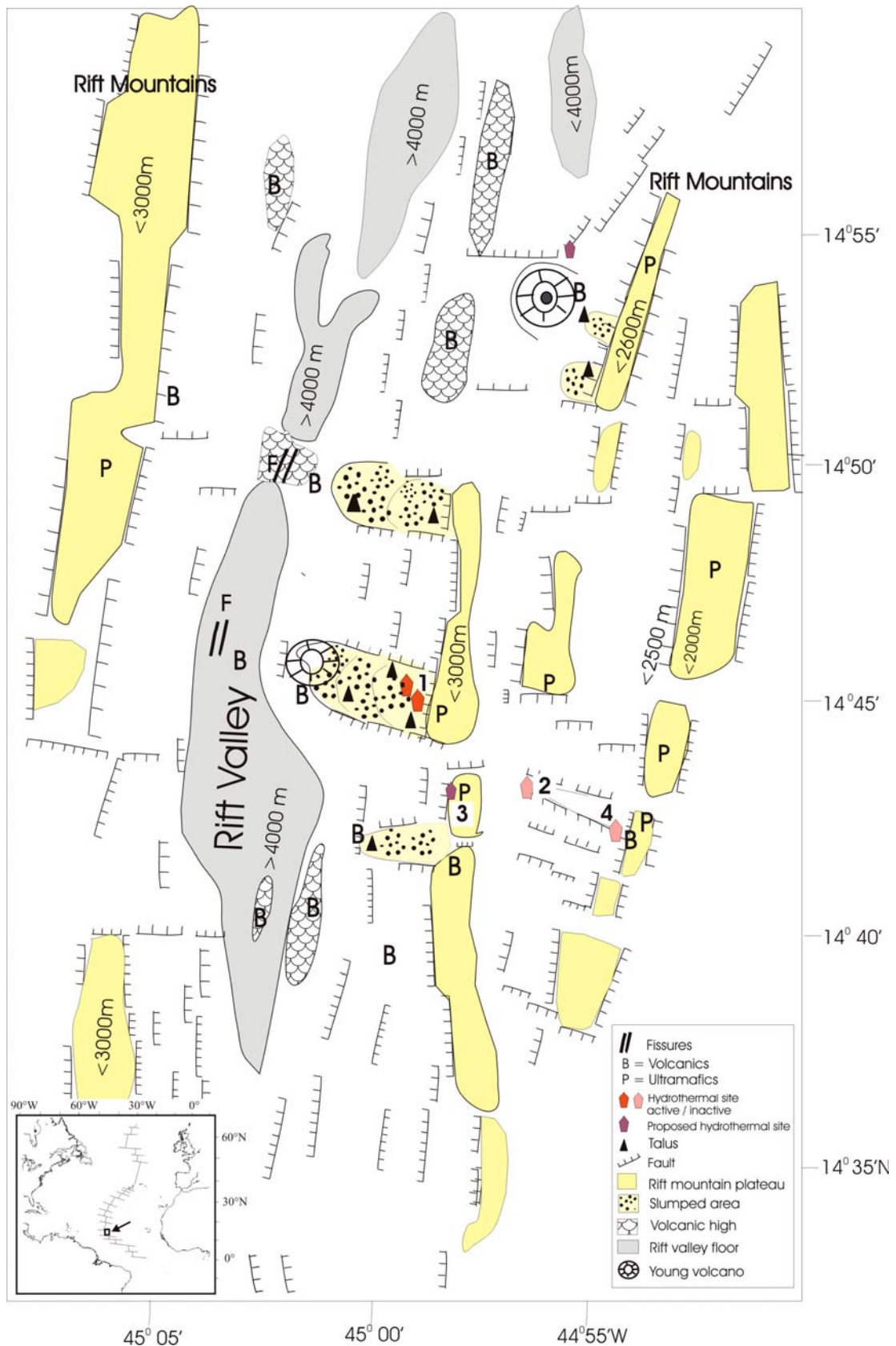


Fig. 3.3: Sketched structural interpretation drawn after multichannel (HYDROSWEEP) bathymetric data of the MAR segment near 14°45'N – 45°00'W obtained during M60/3. Note the cross-cutting faults and the fault-related occurrence of hydrothermal fields. 1, 2, 3, and 4 are separate hydrothermal fields (Logatchev 1-4). Small figure: location of the working area at the MAR.

(Fig. 3.3). The west facing flank of this east rift mountain wall between 2950 m and 3600 m depths consists of several small staircase scarps representing normal faults that are also oriented N013° (Fig. 3.1 and 3.3). Several (3) of these scarps are covered with large „land slides“ forming poorly sorted talus made up of large blocks consisting of mafic and ultramafic rocks (Fig. 3.3 and 3.4). Another OFOS station (84OFOS) carry out along a N-S track on top of the plateau near 14°43'N/44°58.50'W at about 3020 m water depth shows in situ massive ultramafic outcrops. These outcrops extend few hundreds of meters along faulted scarps. Further to the south near 14°41.70'N/44°58'W a volcanic construction made up of pillow lava was seen at about 3000 m water depth.

The rift mountain becomes shallower (1600-2400 m) further to the east with steep faulted scarp culminating with a plateau along longitude 44°52'W (Fig. 3.3). When extrapolating from a TV station (27OFOS), several of these scarps, near 14°42'N/44°52'W at 2700 and at about 2500 m depth, show in situ outcrops of serpentinized peridotite alternated with basaltic flows. This is inferred from the altered debris of metabasalts and other basaltic rocks and serpentinized peridotite recovered at 1608m and 1950 m depths near 14°42.3'N and 44°51.87'W (stations 57 and 63GTV).

The rift mountain walls going from the summit (plateau 2900m depth) of first rift mountain down to the intersection with the rift valley at 3850 m depths consists of several step faulted structures with small relief which are often buried by slumped material. However, during two video camera stations (84- and 89OFOS) large ultramafic blocks were observed and it is not clear whether these large blocks are in place or if they represent down slope transported debris.

#### **3.4.1.4 Off-axis volcanoes**

Two off-axis volcanoes of less than 500 m height were detected during multichannel bathymetric survey (HYDROSWEEP) and observed during deep towed camera stations. They are located on the eastern margin of the rift valley at the intersection with the rift flank located near 14°45'N and 14°55'. They consist of basaltic flows and show recent faulting and collapsed features.

#### **3.4.1.5 Slumped structures**

The presence of irregular bulged features bounded by E-W oriented transverse faults on the eastern rift flank are believed to represent slumped structures as defined from the concentric oval shaped contour lines observed from bathymetry (Fig. 3.3 & 3.4). These features are bounded by “en echelon” faults and form several “step like” terraces bounded by west facing small and semi-circular scarps (<100 m relief) covered with talus material. The terrace and steps extend down to the western slope at the intersection with the rift valley floor. The sizes of these slumped structures vary from about 1 – 4 km in length and 1-2 km in width. The mass-waste forming these slumped structures extends more than 4 km down slope of the eastern wall between 3100 and 3400 m depths (Fig. 3.3 & 3.4). They are covered by pelagic and hydrothermal sediments, with some isolated patches of loose tabular and irregular shaped blocks of ultramafics. The irregular distribution of the sediment and the avalanche debris indicates that the slumping is still an on-going process, probably as the result of major

tectonic events that must have taken place during the uplift of the rift mountains forming the rift valley walls. The ultramafics are believed to represent debris of dislocated material from the rift flank plateau shallower than 3000 m depths bounding the rift valley to the East immediately above the Logatchev hydrothermal field.

Hydrothermal circulation taking place throughout the talus debris has possibly reworked and altered the serpentinized rock fragments. Indeed, sulfur-bearing ultramafic fragments found underneath the hydrothermal chimneys and the surrounding area were collected during several ROV and television grab-sampling stations.

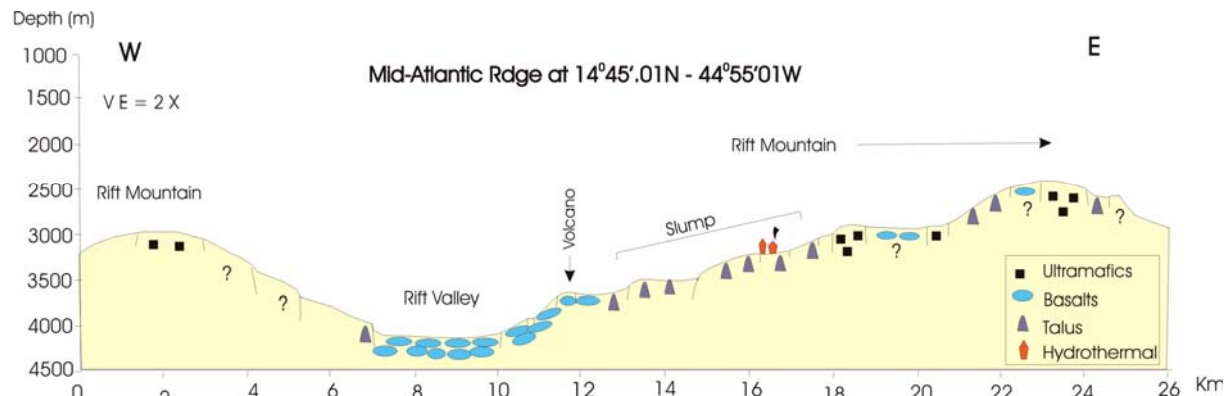


Fig. 3.4 Geological profile (East-West) constructed from bathymetric contour lines at latitudes 14°45.01'N. The geology is inferred from seafloor observations and sampling during cruise M60/03. VE = vertical exaggeration.

### 3.4.1.6 The formation of the Logatchev hydrothermal field

The formation of hydrothermal deposit on top of serpentinized peridotite is believed to result from the circulation of hot fluids through fissured and faulted terrain associated with avalanche debris forming a porous medium (Fig. 3.5). The heat is probably supplied from magma cooling associated with basaltic melts localized underneath the adjacent rift valley and/or off-axis volcanic structures. Also it is not excluded that heat could be provided by localized intrusion of magmatic melts into the peridotite during partial melting. The presence of gabbroic and dolerite fragments with magmatic contacts to the ultramafic rocks indicates late intrusion of magma post dating the emplacement of the serpentinized ultramafics.

## 3.4.2 Geology and morphology of the Logatchev-1 hydrothermal field

(T. Kuhn, K. Schreiber)

The Logatchev-1 hydrothermal field is situated on a plateau right below a 350 m high cliff at a water depth of 3060 m to 2900 m. Mapping and sampling with ROV QUEST and the TV-grab revealed that the field is larger than previously described (Mozgova et al., 1999; Cherkashev et al., 2000; Gebruk et al., 2000). It extends at least 800 m in a NW-SE and 400 m in a SW-NE direction (Fig. 3.2). Even about 600 m to the SW of the main mound hydrothermal precipitates have been detected during a TV-sled track (st. 89; Fig. 3.2 & 3.6). Two main areas of high-temperature hydrothermal activity make up the central part of the

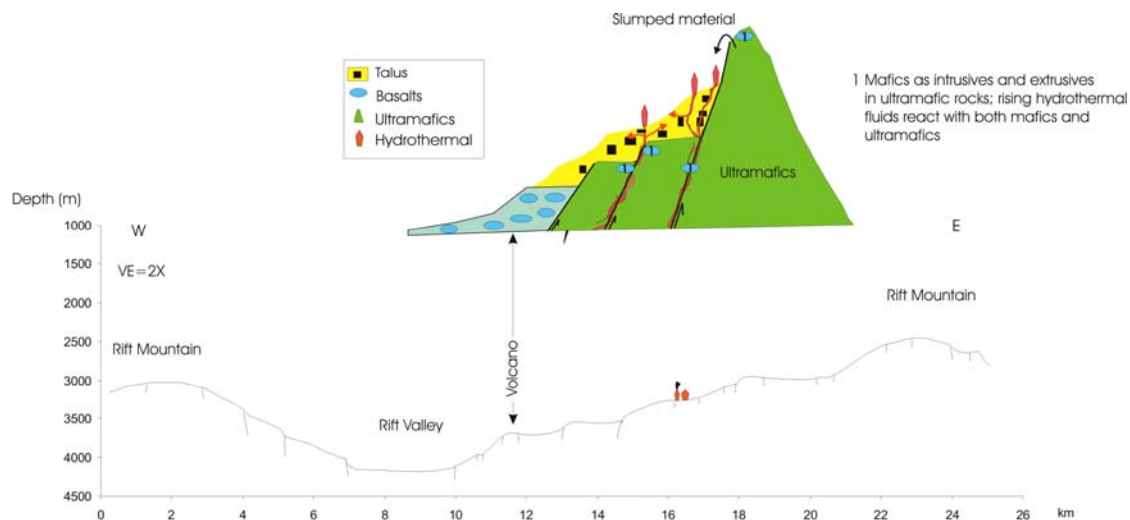


Fig. 3.5 Model for the formation of the Logatchev hydrothermal fields near 14°45'N. The rise of hydrothermal fluids may be partly controlled by fault structures at depth. Fluid-rock reactions may take place within ultramafic and basaltic/gabbroic rocks. Porous talus material formed from large slumpings may provide pathways for large-scale hydrothermal precipitation at and beneath the seafloor. VE= vertical exaggeration.

field: an area of at least three „smoking craters“ (ANNA-LOUISE, IRINA and SITE „B“) and the large mound of IRINA II with black smoker chimneys at its top as well as the newly discovered QUEST smoking crater (Fig. 3.2). The smoking craters show a rim that is 1-2 m high and a 2-3 m deep central depression. ANNA-LOUISE seems to be the largest crater observed having a diameter of about 10 m, whereas IRINA and „B“ have distinctly smaller craters. Up to 2 m high, delicate chimneys are situated on the crater rims. They immediately broke when touched by the ROV manipulators. Black smoke was intensely venting at all three sites, either from the chimneys on the crater rim or from holes in the ground within the craters. At one chimney (the so-called “Candelabrum” at the rim of ANNA-LOUISE) black smoke with both a strong bouyancy but also with nearly no bouyancy (being horizontally dispersed) were observed. Strong bottom currents which changed direction during individual ROV dives resulted in almost horizontal plume dispersal for some black smokers. Dense mussel beds were absent in these environments, and first inspections of the video material revealed that conspicuous hydrothermal fauna was largely restricted to alvinocarid shrimps occurring in moderate numbers, a few crabs (*Segonzacia*), unidentified actinians, the hydrozoan *Candelabrum* and several species of fish (Fig. 3.7). Abundant microbial mats were seen at locations where the black smoke emanating from the sea floor was in regular contact with the surfaces. First inspections of a 3d-model of the seafloor morphology based on ROV depth data suggest that the smoking craters are not sitting on top of a large mound structure but that they rather form single uprisings on the seafloor causing a terrace-like appaerance of an otherwise steep slope (Fig. 3.6).

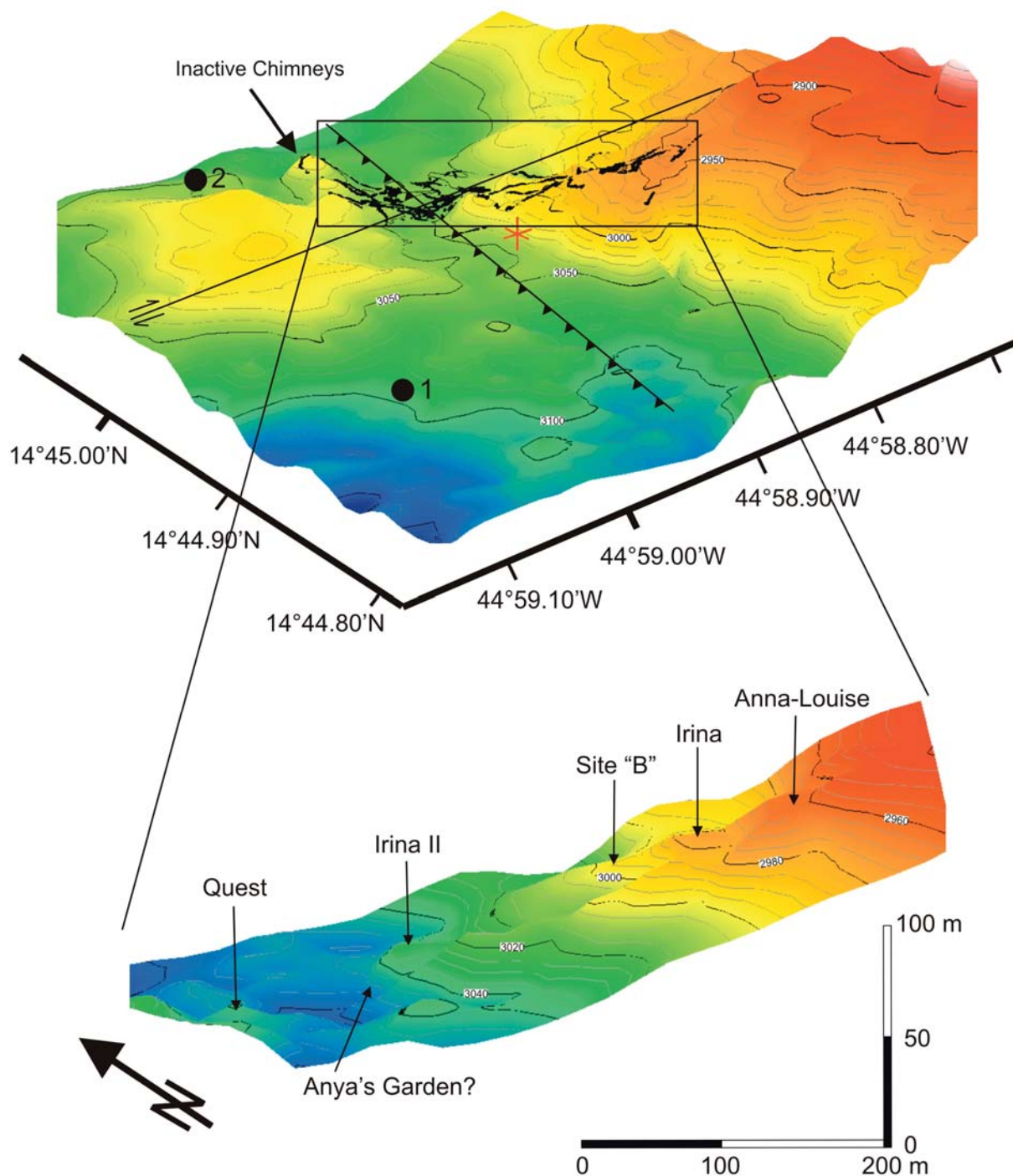


Fig. 3.6 Perspective view of the bathymetry in the vicinity of the Logatchev-1 hydrothermal field based on HYDROSWEEP and ROV data (upper figure). The rectangle marks the outline of the field as known before the cruise M60/3 (Mozgova et al., 1999). Point "1" marks hydrothermal precipitates detected during a TV-sled station, "2" marks low-T precipitates sampled by TV-grab station 82. At this site a T-anomaly of  $0.12^{\circ}\text{C}$  in the near-bottom water was also detected during TV-sled station 22. The normal and transverse faults are interpreted structures (see Fig. 3.3); black lines are ROV dives. The lower picture displays details of the Logatchev field based on ROV depth data. Note that the smoking craters (Anna-Louise, IRINA and Site "B") occur on top of a terrace-like morphology rather than a mound. Both figures are 1.5x vertically exaggerated.

IRINA II consists of a mound with steep slopes rising about 15 m above the surrounding seafloor. The round to elongate structure has a basal diameter of about 60 m. Four vertical chimneys, a couple of meters high, mark the top of the mound. The chimneys are densely overgrown with mussels (*Bathymodiolus* cf. *puteoserpentis*; Fig. 3.7). Shrimps (*Rimicaris exoculata*) gather in large numbers over low-T fluid vents along the sides of the chimneys. The chimneys are surrounded by densely populated mussel beds and also by inactive chimneys and empty mussel shells further down the slope. The Marker ANYA was found on the NW base of the IRINA II slope surrounded by diffuse fluid venting with loosely aggregated mussels, a *Thyasira*-species living in the sediment, and dense clusters of empty vesicomid shells. Living vesicomid specimens were not encountered. However, we doubt that this site is identical to the ANYA'S GARDEN locality described in the literature, because its position and distance from IRINA II does not correspond to the published data (Gebruk et al., 2000). ROV and TV-grab samples revealed that the populations of mussels, crabs and shrimps contained animals of all body sizes, which indicates continuous recruitment of these species rather than recruitment in discrete events, which would produce similar size cohorts.

QUEST is a newly discovered high-T, black smoke venting site situated about 130 m WNW (circa in 330° direction) of the active chimneys of IRINA II (Figs. 3.2 & 3.6). The formation of a depression, small chimneys and smoking pipes emanating black smoke make the QUEST site comparable to the smoking craters on the main mound (Fig. 3.7). However, QUEST does not show the typical circular crater rim and therefore may represent a younger structure, possibly an early state of a developing smoking crater. While the faunal composition grossly corresponded to that found at the smoking craters on the main mound, QUEST additionally harboured scattered clusters of mussels.

Dead mussel beds and/or inactive sulfide structures were mapped about 50 m to the north of the QUEST site, approximately 80 m north of IRINA II, and about 80 m WSW of ANNA-LOUISE. A temperature anomaly of 0.12°C was detected in bottom water during a TV-sled operation close to sampling station 82GTV (Fig. 3.6). The samples recovered from this station contained low-temperature hydrothermal precipitates (Fe-Mn oxides) similar to those generally found in the surroundings of the high-T areas of Logatchev-1.

The position of the Logatchev-1 field may be controlled by two crossing fault structures as suggested by bathymetric and video data (Figs. 3.3 & 3.6). If the seafloor is in fact largely covered by slumped material, the mineralization at Logatchev-1 may form a large stockwork or replacement zone beneath the seafloor (Fig. 3.5). The widespread occurrence of both low-T and high-T precipitates at the seafloor supports this hypothesis which can only be further tested by geophysical investigation (geoelectrics) and by drilling.

Detailed maps of the different hydrothermal structures of the Logatchev-1 field based on ROV tracks are given in Appendix 2.

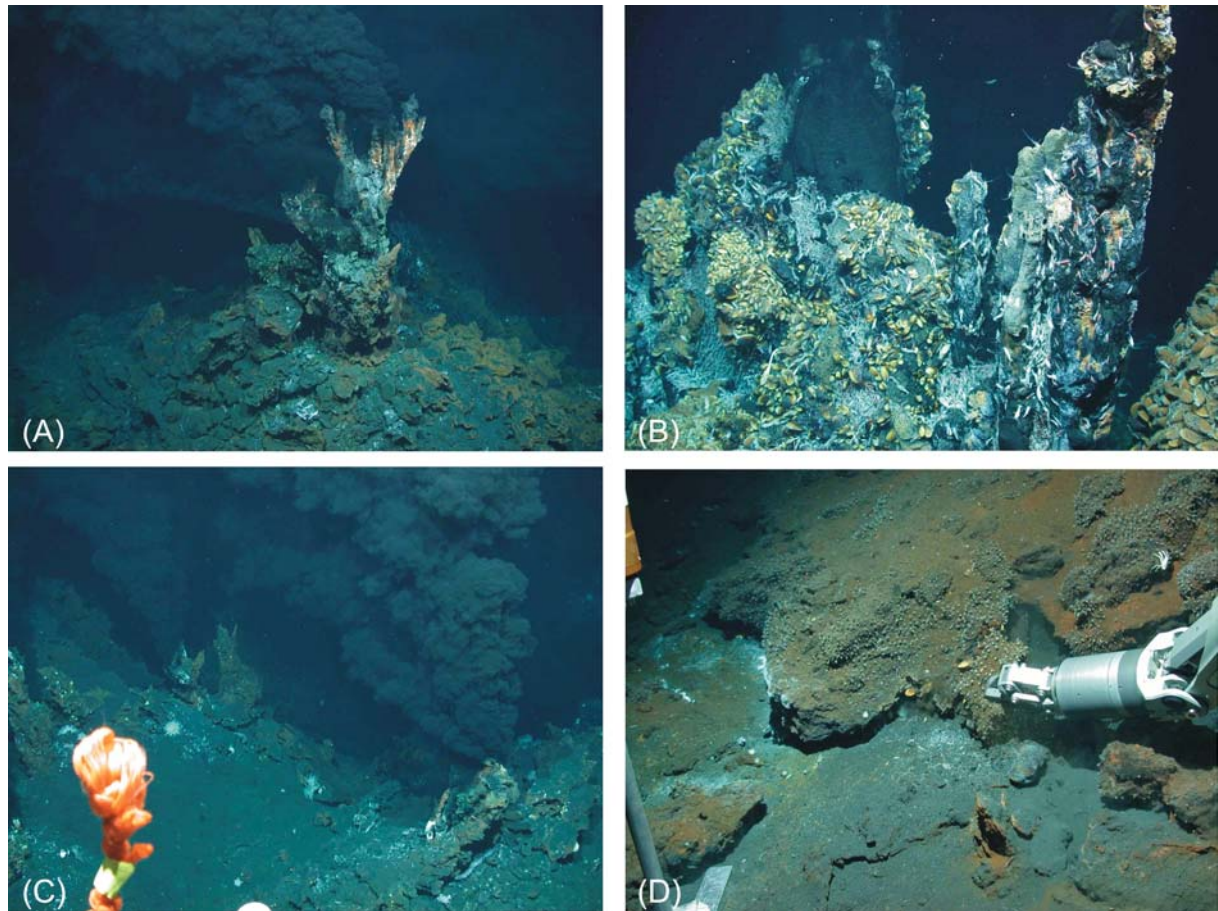


Fig. 3.7 Seafloor photographs from Logatchev-1 field taken with a SCORPIO still camera mounted on the ROV QUEST. (A): The “Candelabrum” chimney on the rim of smoking crater ANNA-LOUISE. (B) Chimney complex at IRINA II. Note the abundant vent fauna compared to (A). (C) Small chimneys in a depression marking the newly discovered QUEST site. (D) Sulfide-rich crusts covering the seafloor near QUEST site. Such crusts were observed all over the Logatchev-1 field.

### 3.4.3 ROV deployments

(T. Kuhn, V. Ratmeyer, C. Borowski, A. Koschinsky)

The Remotely Operated Vehicle (ROV) QUEST was provided by the University of Bremen (MARUM, Prof. Dr. G. Wefer, Dr. V. Ratmeyer) for cruise M60/3. This cruise was the first one during which the ROV QUEST was exclusively used for scientific purposes. Only two test cruises preceded M60/3 and one major task of this cruise therefore was to check the ROV’s ability to meet scientific requirements.

The QUEST system comprises the ROV itself, a control container, a workshop container, a mobile winch with 5000 m 18 mm steal-armored, optical cable for data and energy transmission and a deployment frame. All of these system components were installed on the afterdeck of R/V METEOR (Fig. 3.8).



Fig. 3.8: The ROV QUEST system on the afterdeck of R/V METEOR consists of the ROV itself (middle), a control container (right side), a workshop container (left side) and a mobile winch (front).

QUEST was deployed over the A-frame with a special deployment frame. However, this frame did not effectively prevent the ROV from swinging to the side during deployment. Once the QUEST is in the water it is free-flowing, i.e., it moves independently from the cable which only transmits energy and data. Five to six bouyancy spheres were fixed on the cable at the first 30 m above the device in order to keep the cable upwards away from the ROV. It is only after the fixation of the bouyancy spheres that the ROV starts diving. Therefore, these spheres had to be removed before the ROV can be recovered. This procedure together with the fact that the vessel was not fully manoeuvrable during the last about 100 m of emerging of the ROV to the surface, were the limiting factors for the deployment of the ROV under different sea states. We could deploy the ROV at a swell up to 2-2.5 m. However, our situation was complicated by a crossing swell of about  $90^\circ$  and  $340^\circ$  which caused strong rolling of R/V METEOR.

The ROV sinks with about 0.5 - 1 m/s. Together with the deployment/recovery procedure the submergence to the seafloor and the emergence back to the vessel took 2 hours each for a water depth of 3000 m.

We regularly started our ROV stations at 8:00 a.m. with checking of the system which took about 1 hour. After lowering the ROV to the seafloor at 3000 m water depth we started the work on the seafloor at about 11:00 a.m. and continued working until 17:00 to 21:00 p.m. Between 19:00 p.m. and midnight the ROV was back on deck, the subsamples were taken and the treatment of the samples started. Since most of the water and biological samples had to be worked with immediately after the dives, most of the scientists had to work all night after a ROV station. Routine technical checking was the work of the ROV team after each dive

which took about 1 hour if no technical problem had occurred. If all system components work reliably the next ROV station can start the next morning.

Based on our experience and on a ROV crew of 6 persons it is possible to have two ROV stations with bottom times of 5-7 hours on two successive days and one day for technical maintenance (provided the weather is ok). A careful planning of the ROV stations and of the sample treatment is as necessary as a complementary scientific program to fill the days during which the ROV cannot be deployed.

The navigation of ROV QUEST was realized by two systems: an USBL and a Doppler-Velocity-Log (DVL) navigation. The USBL was realized with the POSIDONIA system from IXSEA OCEANO (Brest, France). At the beginning of all station work a reference station (mooring with a transponder) was set on the seafloor. This station was calibrated by running an Eight over the station with R/V METEOR as requested by the POSIDONIA software. This way the position of the reference station could be calculated with an accuracy of 2-3 m in xy-direction and 1 m in z-direction. To navigate the ROV QUEST on the seafloor a responder was mounted on the frame of the ROV which was electrically triggered. Unfortunately, this responder had an electrical failure during the first dive and could no longer be used. Moreover, it was not possible to trigger the responder in transponder mode, i.e., acoustically through the water column, because the QUEST motors are too noisy. Therefore, a DVL navigation system was applied using a doppler log installed on the ROV. This way, two homer beacons were set on the seafloor and their exact position were calculated using the reference station as a fixed point. It was then possible to calculate every position on the seafloor either with respect to the reference station or to the homer beacons. Navigation within a range of about 500 m around the reference station or beacons was possible. Since we went to the same seafloor structures several times we could control the accuracy of this navigation which turned out to be within a few meters. Problems only occurred when the ROV was sitting on the seafloor for a longer time during experiments or sampling. During such situations a drift of position occurred which had to be recalculated.



Abb. 3.9 Two homer beacons used for ROV QUEST navigation during M60/3.

During each station different data accumulated, including navigation, heading, depth, height above seafloor, video, photo, in-situ sensors, protocols, sampling etc. All data were gathered during each dive in a data base provided by the ROV crew. The navigation data can be synchronized

with all other data via the time frame. This was done after each dive using the software ADELIE which consists of components for the synchronization of data as well as for GIS-based (ARCVIEW) display and analysis.

### 3.4.4 Low-temperature measurements in the Logatchev-1 hydrothermal field

(K.S. Lackschewitz, N. Augustin, H. Villinger)

During the FS Meteor cruise M60/3, first temperature measurements in the Logatchev hydrothermal field were performed. A miniaturized temperature data logger (MTL) was mounted on ROV QUEST to continuously record temperatures during every dive. Additionally, we deployed 4 data loggers at the ocean floor for monitoring temperatures in areas with diffuse fluid outflow and biological colonization. The MTLs were constructed to be extremely robust, small (16 cm long, Fig. 3.10) and easy to operate in water depths up to 6000 m (Pfender and Villinger, 2002). The temperature range extends from  $-5$  to  $+60^{\circ}\text{C}$  with an absolute accuracy of  $\pm 0.1\text{K}$  and a relative temperature resolution of  $0.001^{\circ}\text{C}$ . We increased the absolute accuracy of the MTLs through a precise calibration by comparing the data logger measurements to a high precision thermometer mounted at a CTD. Therefore, we attached 7 MTLs at the CTD and measured a water profile down to 3200 m with the highest sample rate of 1s. The temperature measurement range was 26 to  $3^{\circ}\text{C}$ .



Fig. 3.10 Temperatur logger for low-T hydrothermal fluids used during M60/3.

We measured the temperature distribution in the Logatchev-Field 1 during 8 ROV dives. The data obtained from the MTLs show a background bottom water temperature of approximately  $2.6^{\circ}\text{C}$  which clearly increases in areas with active high-temperature black smokers and craters (Fig. 3.11). The highest measured temperature was  $31^{\circ}\text{C}$  in the near-bottom water close to high-T vents, whereas the average increased temperatures ranged between  $2.7$  and  $3.5^{\circ}\text{C}$ . In addition, numerous diffuse outflow sites were identified. One MTL, which we left for 3,5 days at the seafloor in an area with diffuse fluid-outflow and a colonization of mussels recorded temperature variations between  $2.7$  and  $3.2^{\circ}\text{C}$  (Fig. 3.12). One can clearly observe a periodic change in temperature which is most likely caused by the tidal influence on pressure and/or bottom currents. Temperature measurements on a diffuse vent at the crater rim of IRINA over 3 days revealed pulsating temperatures with variations over time periods of 1 to 2.5 hours. The longer a cycle lasted the higher the temperatures went within a range between  $2.7^{\circ}\text{C}$  and  $8^{\circ}\text{C}$ .

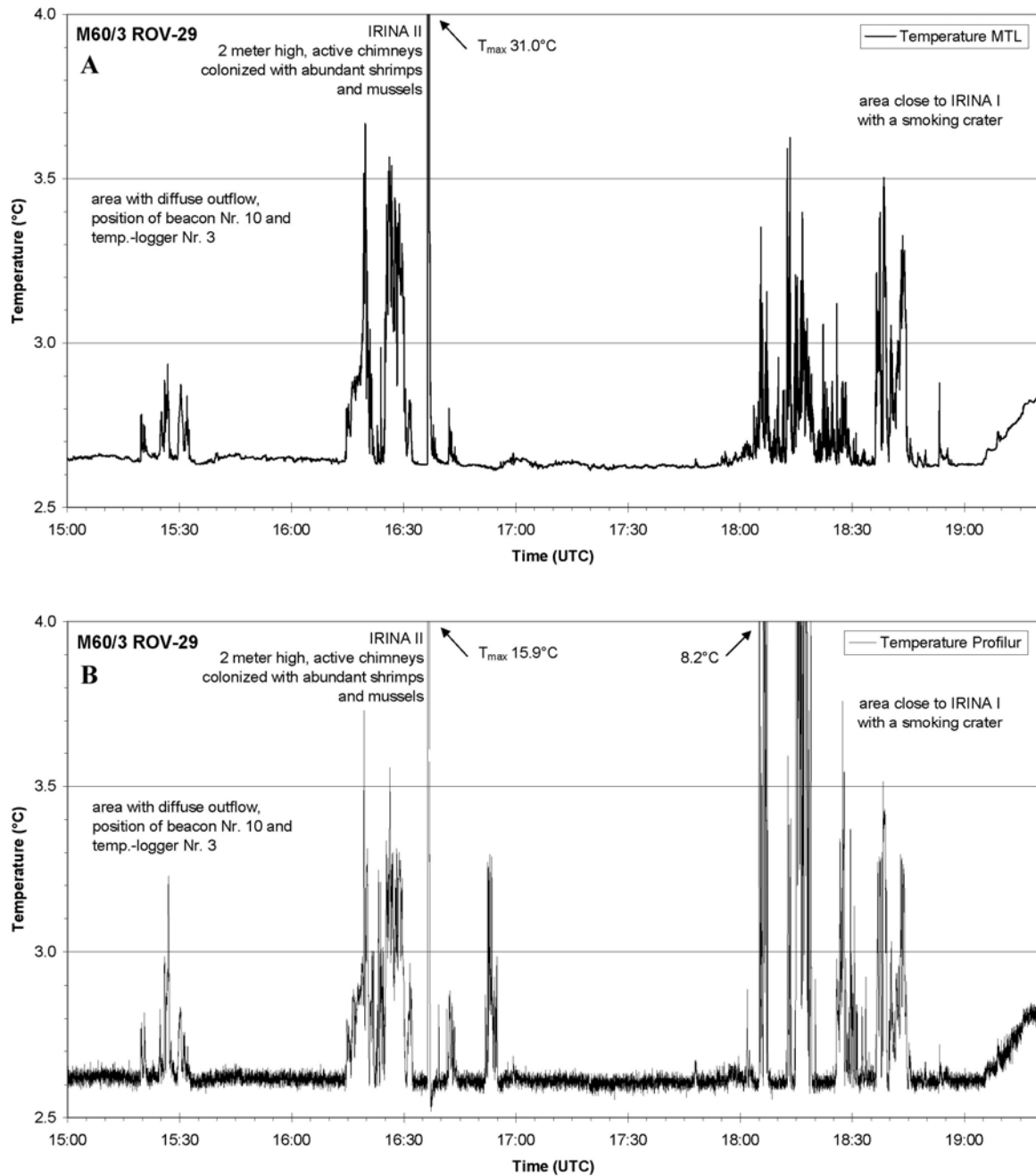


Fig. 3.11 Comparison of temperature profiles recorded during dive 29ROV (see Fig. 3.2). A: Miniaturized Data Logger (MTL). B: PROFILUR, Pt100 sensor. Both sensors were mounted on the tool sled of ROV QUEST.

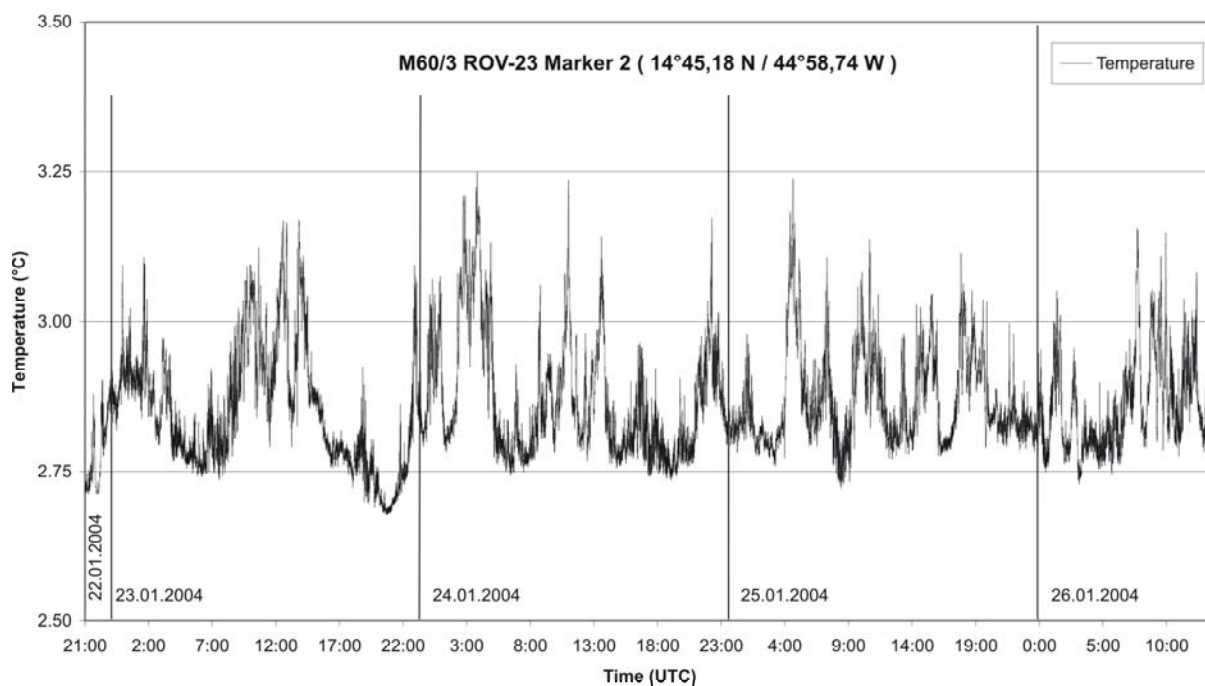


Fig. 3.12 Temperature measurements of a diffuse, low-T emanation site at the mussel bed close to the high-T chimney complex at IRINA II using a miniaturized temperature logger. The logger was placed on top of the mussel bed.

### 3.4.5 *In situ* measurements of biogeochemical parameters: temperature, oxygen, hydrogen sulfide, pH and conductivity

(F. Zielinski, C. Borowski, N. Dubilier)

The mussel *Bathymodiolus puteoserpentis* harbors sulfide- and methane-oxidizing bacteria in its gills and occurs in large quantities at the Logatchev 1 hydrothermal vent field. To obtain a better understanding of the environment of these mussels and how it affects their productivity we collected *in situ* measurements of temperature, oxygen, hydrogen sulfide, pH, and conductivity in the waters surrounding the mussels (Fig. 3.13). The data were gained using sensors and microsensors connected to the PROFILUR, a custom-built pressure- and water resistant titanium cylinder (525 x 145 mm) which houses the electronics for signal- and A/D-conversion. The PROFILUR was tested to withstand pressures up to 4000 m depth and was thus well suited for the demands of the M60/3 cruise. The following sensors were employed: Pt100 temperature sensors, (UST Umweltsensortechnik GmbH, Geschwenda, Germany), Clark type O<sub>2</sub> microsensors (Revsbech 1989), amperometric H<sub>2</sub>S microsensors (Jeroschewski et al. 1996, Kühl et al. 1998), glass pH microelectrodes (Revsbech & Jørgensen 1986) and conductivity sensors. Except for the Pt100 temperature sensor all microsensors were manually produced at the MPIMM, in the Department of Biogeochemistry, Group of Microsensors.

Before each ROV dive the sensors were connected to the PROFILUR electronics by inserting them in plastic holders filled with paraffin oil for pressure compensation. After extended calibrations of all sensors, the PROFILUR was fastened to an extendable drawer underneath the ROV, with the sensors tip protruding from the drawer (Fig. 3.14). All data were stored in the internal PROFILUR memory as well as in the central ROV database and downloaded for later

analysis at the end of the dive. *In situ* measurements with the PROFILUR were carried out on dives 29, 38, 56 and 66ROV. Temperature, H<sub>2</sub>S and O<sub>2</sub> were measured on all 4 dives, pH on 3, and conductivity on 2 of the 4 dives.



Fig. 3.13 The PROFILUR measuring geochemical data at a *Bathymodiolus* mussel colony on the active vent structure of IRINA II.

Temperature measurements were transmitted on board for online temperature tracking. Consistent with the data obtained from the MTL our sensor measured an average bottom water temperature of 2.6°C and an increase in temperature at diffuse outflow sites ranging from 2.7 to 3.5°C.



Fig. 3.14 The PROFILUR mounted on the extendable drawer underneath the ROV set up for the dive to come. The microsensors were protected by a cage.

The temperature profiles of the PROFILUR and MTL were also in good agreement, with both detection methods often showing similar temperature gradients at similar time points (Fig. 3.11). However, the absolute temperature measured at steep gradients often varied between the two methods. In some cases, the PROFILUR measured peak temperatures up to 10-times higher than the MTL. This is most likely due to the different positions of the devices on

the ROV. These were separated from each other by about 1 meter, a distance at which steep temperature gradients can occur at vents. For example, the PROFILUR registered a steep temperature increase while approaching a *Bathymodiolus* mussel colony on an active vent structure with 26.8°C being the highest temperature measured, while the MTL recorded the regular background temperature of 2.6°C at the same time point (Fig. 3.15). All other sensor data are in the process of being analyzed.

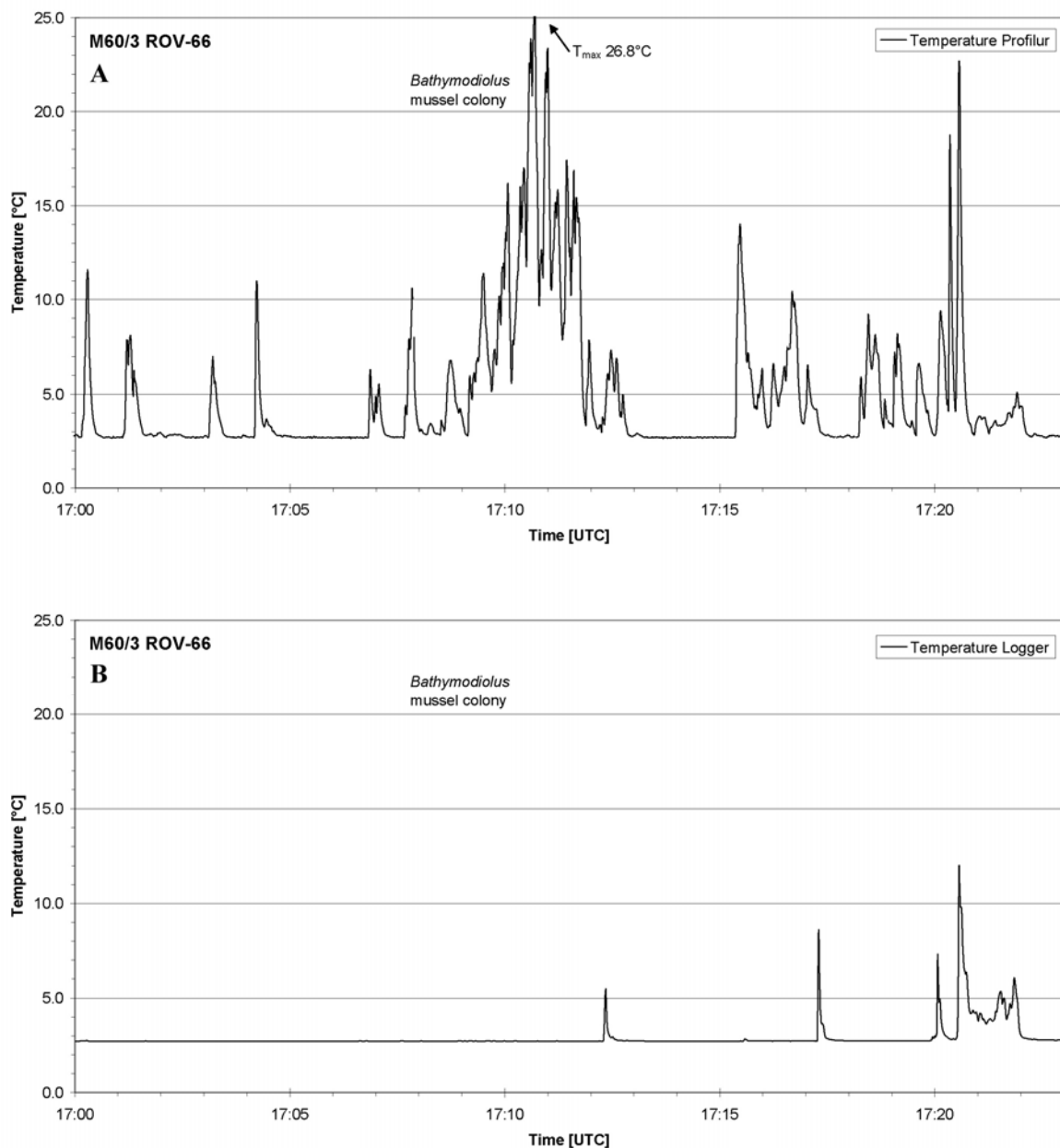


Fig. 3.15 Comparison of temperature profiles at a *Bathymodiolus* mussel colony recorded during dive 66ROV (see Fig. 3.2). A: PROFILUR Pt100 sensor. B: miniaturized data logger. For further explanation see text.

### 3.4.6 OFOS deployment

(T. Kuhn, S. Petersen, K. Schreiber, R. Hekinian)

A total of 14 TV-sled stations were carried out during M60/3 (Tab. 3.1), most of them in the vicinity of the Logatchev-1 hydrothermal field but also on top of the rift mountains, in the rift valley and in Working Area II (Fig. 3.1). The objectives of the OFOS stations were (i) to map the contact between ultramafic and mafic rocks and to recognize if this contact is stratigraphic or tectonic, (ii) to distinguish between talus and outcropping rocks, (iii) to map faults and fissures, and (iv) to measure the near-bottom water temperature in order to detect hydrothermal activity. The IFM-GEOMAR TV-sled was equipped with a BENTHOS photo camera and flash, a SONY digital camcorder and a FSI 3" memory CTD probe. In order to get exact OFOS position data a POSIDONIA transponder was mounted on the TV-sled's frame providing on-line navigation data of both the vessel and the OFOS.

Table: 3.1: OFOS stations during M60/3 (coordinates for the OFOS position at seafloor are given).

Station	Area	Location	Depth	Date	Objective & summary of results
22-OFOS	Logatchev 1	14° 46.61' N 44° 58.23' W to 14° 48.27' N 45° 01.79' W	2708 m to 3597 m	21.01.04	Profile over the Logatchev-1 hydrothermal field and structures along the inner rift valley flank. Talus and sediment mark the field and pillows appear at the flank of the rift valley.
27-OFOS	Logatchev 2	14° 42.30' N 44° 53.87' W to 14° 43.11' N 44° 56.10' W	1615 m to 2650 m	23.01.04	Transect along a WNW-ESE ridge. Ultramafic blocks (mainly talus) and sediments cover the ridge. An inactive mussel field was discovered (Logatchev-4).
40-OFOS	Working Area II	14° 53.43' N 44° 55.04' W to 14° 53.96' N 44° 55.53' W	3221 m to 3330 m	27.01.04	Mapping of Working Area II, search for hydrothermal activity. DVS failure, end of OFOS station due to winch problems.
42-OFOS	Working Area II	14° 54.02' N 44° 55.41' W to 14° 54.90' N 44° 57.33' W	3345 m to 3447 m	27.01.04	Continue mapping of station 40 OFOS in Working Area II, but on a more northerly course. Only basalt along the track, few sheet flows, talus very abundant; missing of the described hydrothermal site.
46-OFOS	Working Area II	14° 54.19' N 44° 55.63' W to 14° 54.43' N 44° 55.62' W	3462 m	28.01.04	Locate hydrothermal field in Working Area II. Only basalt noticed, small pillow mounds & ridges, some larger scarps, crosscutting faults but no hydrothermal activity.
47-OFOS	Working Area II	14° 54.99' N 44° 55.15' W to 14° 54.43' N 44° 55.62' W	2490 m to 3538 m	29.01.04	Investigation of the sea floor in Working Area II. Ultramafics all the way, heavily sedimented; discovery of one large scarp (30 m).
50-OFOS	Arrowhead Area	14° 48.99' N 44° 58.37' W to 14° 50.86' N 45° 03.25' W	2820 m to 3840 m	29.01.04	Mapping the contact of ultramafics to basalts. At the eastern flank of the rift valley, east of the rift, axis only ultramafics occur. Rift axis consists of a succession of undulating hills cut by 3 fissures.
60-OFOS	Logatchev 1	14° 44.38' N 44° 58.30' W to 14° 45.61' N 45° 58.21' W	2758 m to 2970 m	01.02.04	Mapping the plateau above Logatchev 1 field trying to locate areas of hydrothermal activity. The plateau consists of a highly sedimented area without any traces of hydrothermalism.
61-OFOS	Area W of	14° 45.10' N	3049 m	01.02.04	Mapping the contact between basalts

Station	Area	Location	Depth	Date	Objective & summary of results
	Logatchev 1	44° 59.40' W to 14° 45.65' N 45° 01.35' W	to 3835 m		and ultramafics as well as a small volcanic feature west of Logatchev-1. The eastern valley wall consists of ultramafics, which is followed by talus. The volcano is made up of rather young pillow basalt.
<b>70-OFOS</b>	Central Valley	14° 44.63' N 44° 01.25' W to 14° 47.60' N 45° 03.55' W	3889 m to 3623 m	04.02.04	Mapping the Central Valley floor looking for tectonic/volcanic activity. Basalt crops out along the whole track with low sedimentation pointing to recent volcanic activity.
<b>72-OFOS</b>	Central Valley	14° 46.36' N 44° 57.80' W to 14° 49.02' N 45° 00.83' W	2770 m to 3946 m	05.02.04	Mapping the eastern wall of the rift valley. A large scarp > 100 m vertical offset in ultramafics. Ultramafics all along the track.
<b>80-OFOS</b>	Central Valley	14° 39.72' N 44° 59.48' W to 14° 40.71' N 45° 02.77' W	3481 m to 3976 m	06.02.04	Mapping the eastern flank of the Central Valley at station 17 CTD (prominent CH <sub>4</sub> anomaly) and across the axial valley. Young pillow basalts all the way along the track. Abundant fissures marking active tectonics at the western wall.
<b>84-OFOS</b>	Logatchev and Central Valley	14° 43.48' N 44° 58.47' W to 14° 42.38' N 45° 59.91' W	2939 m to 3896 m	07.02.04	Mapping of the seafloor at Logatchev-3. No T anomaly found. Sharp contact between ultramafics and basalts close to the kink of the track (see Fig. 3.1)
<b>89-OFOS</b>	Area SW of Logatchev 1	14° 45.15' N 44° 58.84' W to 14° 44.91' N 45° 58.85' W	3011 m to 3090 m	08./09.02. 04	Mapping of the area Southwest of Logatchev-1. Abundant scarps, fissures and only ultramafics along the whole track.

Most of the results of the OFOS deployment are already discussed in chapter 3.4.1. With respect to the main objectives given above, the following results can be stated:

- (i) The central valley floor is mainly covered by rather young basaltic flows, whereas most of the eastern inner flanks of the rift valley are made up of ultramafic rocks. However, mafic rocks were also sampled from the flanks but seem to be of minor importance. Magmatic contacts were observed in some samples from the flanks (e.g., 49GTV-2; see chapter 3.4.7). Since the ultramafic rocks emplaced tectonically, there should be a tectonic contact between ultramafic and mafic rocks. This contact is mainly situated at the lower part of the inner flank close to the morphological transition from the slope to the rift valley floor. However, this contact is often blurred by talus material. Larger outcrops related to basaltic volcanism appear only at two locations higher up the flanks where young basalt volcanoes are located (see Fig. 3.3).
- (ii) Large parts of the eastern valley flanks are covered by talus material. This is especially true in the vicinity of the Logatchev-1 hydrothermal field.
- (iii) Sites of active tectonics may be characterized by open fissures, nearly vertical escarpments with no sediment coverage and tectonically deformed rocks. Open fissures were found in the middle of the central valley at the end of station 50OFOS in basaltic flows (at 14°50.1'N / 45°01.5'W, Fig. 3.1). This position may mark the current spreading axis which may be in a phase of tectonic spreading. Almost vertical walls without sediment coverage in ultramafic rocks were mapped in water depths between 3300 and

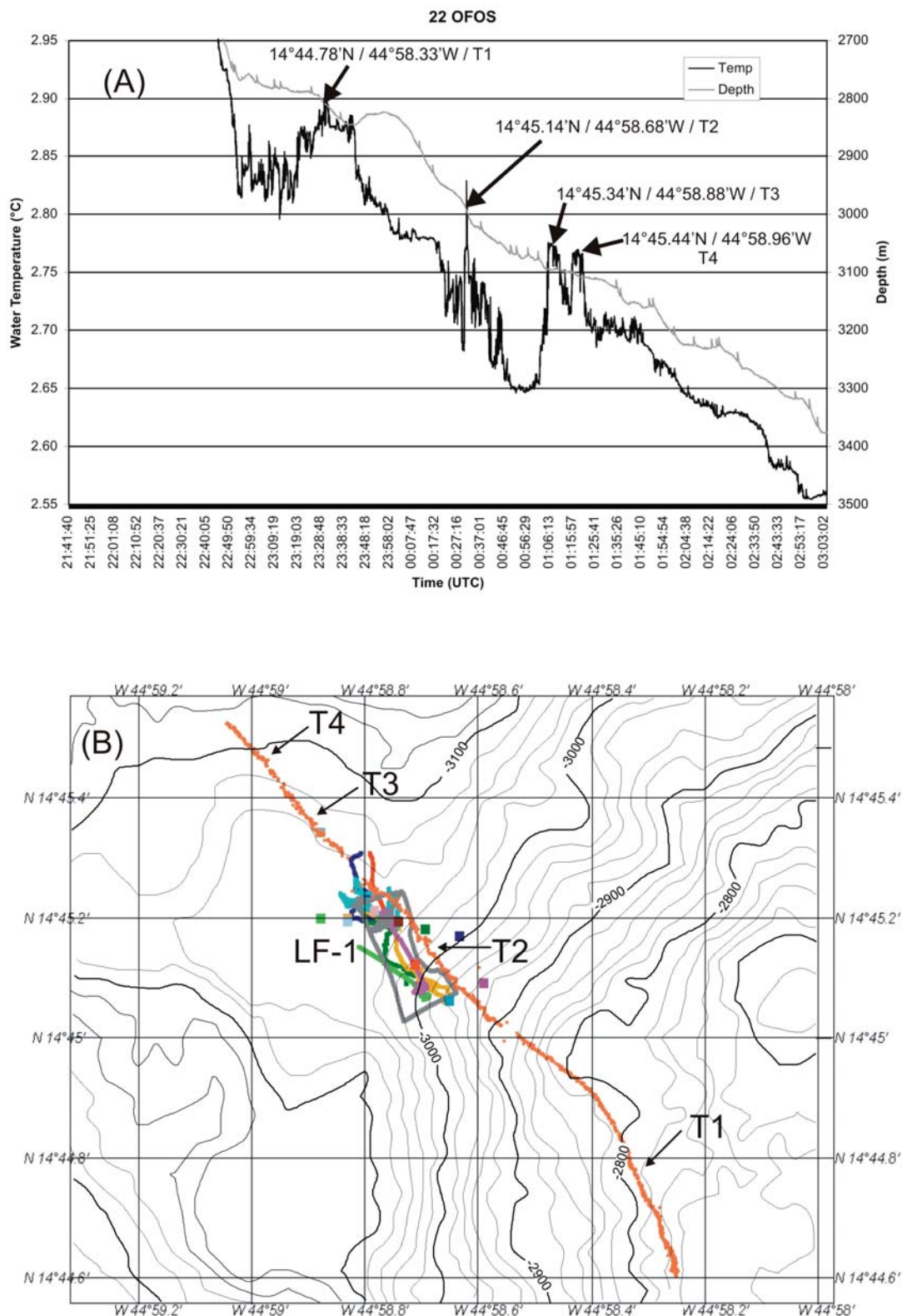


Fig. 3.16: A: Part of the water temperature and depth vs. time diagram of OFOS station 22 showing four distinct T anomalies between 0.07 and 0.13 °C. B: Track of 22OFOS in the vicinity of the active Logatchev-1 hydrothermal field (LF-1; see Fig. 3.2). Three T anomalies occur outside the LF-1 field. T 3 and 4 suggest that LF-1 may be distinctly larger than previously known, T1 may indicate another active hydrothermal field.

3600 m all along the inner eastern rift flank in stations 47, 72, 22, 61, 89 and 84 (Fig. 3.1). These steep slopes seem to mark the active tectonic emplacement of the mantle rocks. Indications of active tectonics were also mapped in working area II along stations 42 and 46OFOS. Tectonically deformed ultramafics with mylonitic textures were sampled in working area II (49GTV) at a position which is situated along the track of 47OFOS. OFOS station 27 was carried out on a WNW-ESE striking ridge, the southern slope of which is also characterized by almost vertical scarps of some tens of meters vertical offset. The Logatchev-4 hydrothermal field is situated on this tectonic structure (Figs. 3.1, 3.3).

(iv) Increased bottom water temperatures were only found during station 22OFOS which crossed the active Logatchev-1 hydrothermal field (Fig. 3.16). Four T anomalies occur close to the Logatchev-1 field, one marks the field itself whereas three others indicate either a considerable larger areal extent of the Logatchev-1 field or yet undiscovered new hydrothermal fields.

### 3.4.7 Sample description

(S. Petersen, K. Lackschewitz, N. Augustin, L. Franz, R. Hekinian, D. Birgel)

#### 3.4.7.1 Summary

During cruise M60/ 3 a total of 5 ROV dives and 16 TV-grab stations recovered geological samples from the seafloor. Detailed information on the sampling stations are given in Table 3.2.

Host rocks of the Logatchev field are mainly serpentized peridotites while basalts and gabbros (sometimes in magmatic contact with peridotite) occurred subordinately. Remarkable are samples of coarse grained websterites, orthopyroxenites and orthopyroxene-rich, pegmatoidal norites, which are interpreted as magmatic cumulates from the crust/mantle transition zone. A large variety of hydrothermal samples were recovered including active and inactive massive chalcopyrite chimneys, massive sulfides, silicified breccias and crusts, soft and indurated hydrothermal sediments, abundant secondary Cu-sulfides, red and orange jaspers, abundant Fe-Mn-oxyhydroxides as well as atacamite and Mn-oxides. Three grabs recovered silicified crusts that may act as a cap rock allowing for conductive cooling of the hydrothermal fluid. Sulfides are enriched immediately underneath this cap rock and usually contain a more pyrite-rich section at the top followed by more Cu-rich sulfides (chalcopyrite and isocubanite) underneath. The base of the grabs commonly contained large amounts of gray to green-gray indurated mud related to alteration of host rock material. This suggests that the massive sulfides along the flanks of the deposit might only be a thin veneer directly at or below the seafloor. The amount of sulfide talus, the state of oxidation and the widespread abundance of atacamite suggest an old active hydrothermal system. While oxidation is common, local reducing conditions result in the formation of secondary Cu-sulfides, mainly chalcocite and minor bornite and digenite, and rare native copper. Overall, the sulfides at the Logatchev 1 hydrothermal field are extremely enriched in Cu over Zn when compared to other seafloor hydrothermal systems.

### 3.4.7.2 Descriptions of individual stations

**23ROV:** During this dive silicified crusts with abundant pyrite were recovered from the northwestern end of the Logatchev 1 field (sample 23ROV-10) near the newly found Quest hydrothermal site. The sample is irregular in shape and consists of abundant amorphous silica with disseminated pyrite and white, angular, altered rock fragments. Later in the dive two pieces of a group of inactive black smoker type chimneys southwest of IRINA II were sampled in the vicinity of a mussel bed (samples 23ROV-12 and 23ROV-13). Piece 23ROV-12 consists of a 10 cm thick chalcopyrite core with a 1-7 cm rim of sphalerite-rich material. The outer crust is coated by Fe-Mn-oxyhydroxides. The whole sample seems to be silicified. Sample 23ROV-13 is a multi-spired chimney with a curved outline. At least three generations of chimney growth are visible. Two different sample groups were recovered on the sample tray or in the ROV frame and their sampling location is therefore uncertain. Samples 23ROV-14 are two pieces of light-brown Fe-oxyhydroxides with some black Mn-oxide layers. Samples of station 23ROV-15 are irregular dark-brown to red Fe-oxyhydroxides coating black to dark gray secondary Cu-sulfides, likely dominated by chalcocite.

Station **26GTV** was attempted in the Logatchev 1 field, but failed, due to an electric failure. However, the grab recovered 5 small ultramafic samples in one of the pipes of the grab. These samples were slightly to almost completely serpentinized harzburgites (26GTV-1,-2,-3; 26GTV-5) and one coarse grained orthopyroxene-websterite (26GTV-4).

Station **32GTV** was attempted on the northern flank of the main mound between the smoking craters to the south and the IRINA II site. The TV-grab recovered several 100 kg's of muddy material with abundant Fe-oxyhydroxides crusts and atacamite (32GTV-1; Fig. 3.17h) at the surface overlying mainly altered wallrock, i.e. strongly serpentinized peridotite (32GTV-3A), peridotite with quartz and sulfide impregnation (32GTV-3D) and orthopyroxene-websterite (32GTV-3B,-3C). Few pieces of massive, fractured quartz were found (32GTV-2) together with a single piece of fine-grained pyrite (32GTV-3E) and some sulfide mud (32GTV-5).

Another TV-grab was performed on the southeastern side of the main mound (station **33GTV**) and recovered Fe-oxyhydroxides with abundant atacamite (33GTV-18) as well as a suite of relatively pristine ultramafics. These were medium- to coarse-grained harzburgites (33GTV-2,-3,-5,-9,-10,-12,-13,-14,-15), coarse-grained to pegmatoid orthopyroxene-websterites (33GTV-7,-8,-8A,-16; Fig. 3.18a,b), several serpentinized peridotites with random orientation of the minerals (33GTV-4,-17), one sheared peridotite mylonite (33GTV-11; Fig. 3.18d) and one medium-grained norite (33GTV-1; Fig. 3.18g). Individual orthopyroxene crystals of the pegmatoid samples reached up to 15 cm in size.

Station **35GTV** was targeted on the large mussel bed in the vicinity of the IRINA II site. The TV-grab sampled abundant fauna including mussels, crabs, snails, and ophiurids. This faunal assemblage lived on a silicified crusts that protected them from the underlying hot fluids. The TV-grab broke this cap rock seal and all mussels were subsequently cooked during ascend. In situ temperatures measured in the mud underneath the crust ranged from 96-106°C. The geological samples recovered include the silicified cap rock (35GTV-1, up to 20 cm thick; Fig. 3.17d) which contains altered and fresh wallrock fragments and orthopyroxene crystal pieces as well as sulfide fragments. Underlying this crust is a section of porous to massive chalcopyrite and isocubanite (35GTV-2; Fig. 3.17e). Few pieces of pyrrhotite-rich

Table 3.2: Geological samples taken during cruise M60/3

Station	Date	Time	Lat. / Long.	Depth	Comment
23ROV-10	22.01.04	21:35	14°45.209'N/ 44°58.823'W	3038 m	siliceous cap rock with sulfides
23ROV-12	22.01.04	22:28	14°45.187'N/ 44°58.747'W	3036 m	inactive chimney
23ROV-13	22.01.04	22:28	14°45.187'N/ 44°58.747'W	3036 m	inactive chimney
23ROV-14	22.01.04	no data	location uncertain	no data	Fe-oxyhydroxide chips
23ROV-15	22.01.04	no data	location uncertain	no data	secondary Cu-sulfides, small bits
26GTV	23.01.04	13:13	14°45.19'N/ 44°58.77'W	3024 m	serpentinized harzburgite and Opx-websterite
32GTV	25.01.04	12:46	14°45.12'N/ 44°58.71'W	2982 m	Fe-oxyhydroxides, atacamite, sulfide sand, Opx-websterite and serpentinized peridotite
33GTV	25.01.04	17:28	14°45.06'N/ 44°58.65'W	2921 m	Fe-oxyhydroxides, atacamite, norite, harzburgite, websterite and peridotite
35GTV	25.01.04	23:38	14°45.19'N/ 44°58.74'W	3019 m	106°C on deck, mussel bed, massive sulfides, serpentinite, harzburgite
49GTV	29.01.04	16:25	14°55.48'N/ 44°54.34'W	3344 m	serpentinized dunite, harzburgite, microgabbro and basalt
53ROV-1	30.01.04	16:19	14°45.181'N/ 44°58.741'W	3033 m	black smoker chimney talus
53ROV-13	30.01.04	20:37	14°45.083'N/ 44°58.710'W	2959 m	black smoker chimney talus
53ROV-15	30.01.04	no data	location uncertain	no data	porous chalcopyrite/pyrrhotite
53ROV-16	30.01.04	no data	location uncertain	no data	red jasper
54GTV	31.01.04	02:39	14°45.17'N/ 44°58.63'W	2940 m	sulfide-carbonate breccias, jasper, atacamite, native copper
56ROV-1	31.01.04	no data	14°45.188'N/ 44°58.739'W	3034 m	pyrrhotite-rich chimney
57GTV	01.02.04	03:13	14°42.29'N/ 44°53.67'W	1608 m	serpentinized and brecciated peridotite, amphibolite and basalt
62GTV	02.02.04	02:07	14°45.20'N/ 44°58.83'W	3037 m	100°C on deck, silica crusts, sulfides, peridotite and pyroxenite
64ROV-1	02.02.04	17:22	14°45.065'N/ 44°58.691'W	2949 m	black smoker chimney talus
64ROV-2	02.02.04	17:40	14°45.065'N/ 44°58.689'W	2948 m	black smoker chimney talus
64ROV-10	02.02.04	18:38	14°45.068'N/ 44°58.688'W	2949 m	small bits taken with slurp gun
64ROV-11	02.02.04	18:55	14°45.065'N/ 44°58.692'W	2948 m	inactive chimney
67GTV	04.02.04	01:51	14°42.30'N/ 44°54.41'W	1967 m	serpentinized peridotite, orthopyroxenite and metabasalt
73ROV-1	05.02.04	18:30	14°45.197'N/ 44°58.774'W	3050 m	serpentinite and harzburgite
73ROV-2	05.02.04	19:02	14°45.190'N/ 44°58.755'W	3032 m	pyrrhotite-sphalerite chimney
74GTV	06.02.04	01:28	14°45.09'N/ 44°58.59'W	2882 m	carbonate mud with Fe-oxyhydroxides, harzburgite, websterite &

Station	Date	Time	Lat. / Long.	Depth	Comment
77GTV	06.02.04	14:27	14°45.18'N/ 44°58.80'W	3019 m	serpentinized peridotite carbonate mud with Fe- oxyhydroxides, mylonitic serpentinite
78GTV	06.02.04	17:51	14°45.19'N/ 44°58.88'W	3005 m	abundant Mn-oxide crusts, ortho- pyroxenite, websterite, serpentinite
79GTV	06.02.04	20:48	14°45.18'N/ 44°58.69'W	3005 m	Fe-Mn-oxide crusts with atacamite in pelagic sediment
82GTV	07.02.04	13:36	14°45.34'N/ 44°58.88'W	3058 m	Mn-Fe-oxide layers and crusts, talc- bearing serpentinite
83GTV	07.02.04	17:15	14°45.21'N/ 44°58.78'W	3019 m	silica crusts, massive sulfides, Fe- oxyhydroxides serpentinite
87GTV	08.02.04	13:20	14°44.00'N/ 44°58.25'W	2967 m	gabbronorite, melanorite, serpentinized peridotite

material (35GTV-3), of anhydrite (35GTV-7), and of bornite/chalcocite-rich material likely replacing the massive chalcopyrite (35GTV-8) were also recovered. Host rocks include small, altered ultramafic rock chips (35GTV-4), however, larger samples of altered and pyritized harzburgite (35GTV-5) and serpentinite (35GTV-6, 35GTV-9) were also sampled. Remarkable was the presence of a mm-thick norite vein cutting through peridotite sample 35GTV-9. Fe-oxyhydroxide crusts are abundant (35GTV-10).

Station **49GTV** aimed to sample the host rocks of working area II. The collected rocks were mainly ultramafics, which could be discriminated into 5 different groups. Most abundant were slightly serpentinized dunites and harzburgites with mylonitic textures (49GTV-3A to -3C) and with randomly oriented textures (49GTV-3D to -3P). Most of these samples were olivine-rich and display angular to rounded shapes classifying them as part of the talus. The second group is made up of ultramafics with low modal amounts of olivine and laminar to layered silicic melt intrusions (49GTV-4A to -4H; Fig. 3.18f). The third group is formed by distinctly serpentinized dunites and olivine-rich harzburgites with serpentine- and carbonate-filled fractures (49GTV-1A and 1B and 49GTV-5A to -5P). The fourth group consists of penetratively serpentinized peridotites (49GTV-6A to -6F). One rounded dunite sample with an orthogonal, serpentine-filled fracture system (49GTV-2) may be regarded as a magmatic cumulate. Furthermore, one small sample of vesicular basalt (49GTV-7), one basalt with magmatic contact to peridotite (49GTV-8) and one microgabbro (49GTV-9) were found. The matrix to these samples consists of grayish mud (49GTV-10).

**53ROV**: Sample 53ROV-1 is a piece of a chimney wall taken at the small, active black smoker a few meters south of IRINA II and consists of massive chalcopyrite with dots of hematite replacing chalcopyrite. Additionally, talus-like pieces of red jasper beneath a black smoker at the eastern rim of the smoking crater "B" (sample 53-ROV-2) were sampled. Sample 53ROV-13 is a talus piece of a chimney wall that was recovered beneath an active black smoker at IRINA (Fig. 3.17b). The chimney wall seems to be very young and consists entirely of chalcopyrite showing multiple layers resembling tree rings. Sample 53ROV-14 was taken at the base of the same black smoker in bright red Fe-oxyhydroxides. Two samples were recovered on the ROV frame and their sampling location is therefore uncertain. Sample 53ROV-15 is a piece of porous chalcopyrite/pyrrhotite, whereas sample 53ROV-16 is a red jasper.

Station **54GTV** sampled 200 kg of breccia material on a hydrothermal mound to the east of IRINA II. The material consists of secondary Cu-sulfides with cm wide veins of white to brown carbonate + Fe-oxyhydroxides + atacamite + silica (54GTV-2; Fig. 3.17f). Chalcocite seems to be the dominant Cu-sulfide (54GTV-1), however, few relics of primary chalcopyrite are still present (54GTV-3). Native copper occurs as small (< 1mm) specs in the carbonate veins, but also in small late veins of quartz or amorphous silica. Partial oxidation results in the formation of porous, bright red Fe-oxides cementing and replacing chalcocite (54GTV-4; Fig. 3.17g). The surface material contains abundant Fe-oxyhydroxide mud (54GTV-7) and crusts with bright green atacamite (54GTV-6) as well as few large blocks of orange jasper (54GTV-5).

**56ROV**: During this dive a single small piece from an active chimney of IRINA II was accidentally recovered by the PROFILUR system. It consists of fine-grained chalcopyrite-pyrrhotite with a mm thin pyrite/marcasite crust.

Station **57GTV** aimed to sample rocks at the shallowest position near the new Logatchev 4 field. About 50 % of the samples recovered were serpentinized peridotites, i.e. medium-grained dunites and harzburgites (57GTV-1A-1 to -5; Fig. 3.18c), cataclastic, medium-grained peridotite breccias (57GTV-1B-1 and -1B2) and one mylonitic peridotite (57GTV-1C). All these rocks yielded high amounts of relatively fresh olivine crystals. Mafic rocks of this station were pristine, gray-black as well as heavily weathered, brownish vesicular basalts with a dense matrix and mm-sized olivine phenocrysts (57GTV-3A to -3H). A remarkable finding of this grab was a fine-grained, greenish, schistose amphibolite consisting of distinctly aligned hornblende, olivine and plagioclase (57GTV-2). This rock exhibits a mm-sized alteration crust of limonite as well as limonite on fractures.

Station **62GTV** sampled hydrothermal crusts in the Logatchev 1 field and almost exclusively grabbed scoriaceous, black, sulfide-cemented breccias (~100 kg; 62GTV-5). This material contained fragments of the wall-rock and abundant orthopyroxene crystals. The sulfides were predominantly pyrrhotite and subordinately pyrite/chalcopyrite. Ultramafic samples included serpentinized harzburgites with pyrrhotite mineralization on fractures and in the matrix (62GTV-1, -2, -4) and an almost totally serpentinized dunite with a thin sulfide crust (62GTV-3). Few pieces of pyrrhotite-rich material (62GTV-6) contained abundant barite and fragments of heavily altered orthopyroxene. Furthermore, one piece of vein quartz (62GTV-7), gray-green silicified clay (62GTV-8) and dark-brown to red globigerina clay (62GTV-9) were sampled.

**64ROV**: All samples taken during this dive were recovered from the rim of the ANNA LOUISE smoking crater. Sample 64ROV-1 is a massive, porous chalcopyrite-rich chimney with very small conduits and was taken from the talus pile between the active "Candelabrum" black smoker chimney and an inactive chimney next to it, both on the southern rim of the crater. The center of the chimney piece is slightly recrystallized. The outer surface is coated by a thin layer of Fe-oxyhydroxides. A second talus piece of massive, zoned chalcopyrite was recovered from the base of the "Candelabrum" chimney itself (64ROV-2) and shows bulbous chalcopyrite growth on the inside. The zonation is similar to that of sample 53ROV-13. Atacamite occurs on fractures. The middle part of the inactive chimney to the west of the "Candelabrum" black smoker was later recovered (64ROV-11) and consists of massive chalcopyrite with a thin outer rim where chalcopyrite is replaced by bornite. Talus material

from another small, active black smoker on the eastern crater rim of ANNA LOUISE was recovered with the slurp gun (64ROV-10). The sample consists of bright red, oxidized sulfides with remnants of secondary Cu-sulfides, as well as small chips of chalcopyrite and few pieces of sphalerite+anhydrite. Fluid samples were taken at this small black smoker during this dive.

At station **67GTV** two different types of peridotites were recovered: the first group (67GTV-1A,B) consists of coarse-grained to pegmatoid orthopyroxenites with random orientation of the cm-sized orthopyroxene prisms. In part, olivine-rich sections were present. The second group (67GTV-2A to -2K; Fig. 3.18e) comprises distinctly serpentinized, medium- to coarse-grained peridotites, which are strongly fractured. In most cases, the 1-2 mm-wide fractures are filled with serpentine while one sample is cut by a 5 mm-wide talc- and quartz-bearing vein (67GTV-2B). Another suite of rocks (67GTV-3A1,-2,-3) sampled during this station consisted of greenish metabasalts, which in part displayed chilled margin textures. One sample (67GTV-3A3; Fig. 3.18h) displays distinct silicification and a magmatic contact to a coarse-grained ultramafic rock. The metabasites show mm-thick Mn-oxide crusts.

**73ROV**: Ultramafic rocks were recovered from a small outcrop near marker "C". The samples consist of strongly limonitized, reddish serpentinite (73ROV-1A1,2,-1B2) and one sample of coarse-grained, serpentinized harzburgite with a cm-thick, brownish alteration crust (73ROV-1B1). Piece 73ROV-1B2 is cut by several tiny quartz veins. Later in the dive, a dm high, pipe-like sulfide spire was sampled on the eastern side of the venting IRINA II complex (sample 73ROV-2). The spire was one of the few that were not covered by biota and consists of a porous mixture of pyrrhotite and sphalerite.

The aim of station **74GTV** was to sample the sedimented area close to the Logatchev 1 mound. The host-rock found here consists of strongly fractured and distinctly weathered orthopyroxenite and websterite (group 74GTV-1; 15 samples) and peridotites with strong to complete serpentinization (group 74GTV-2; 10 samples). Weakly indurated, brownish-yellow sediment consists of carbonate with globigerina detritus, clay, Fe-oxides/hydroxides and stains of atacamite (groups 74GTV-3, -4, -5).

Station **77GTV** sampled ultramafics to the west of IRINA II in the Logatchev 1 field. One mylonitic, partly serpentinized dunite shows mm-sized olivine porphyroclasts in a dense matrix of serpentine (77GTV-1A). The sample is characterized by a dark-grayish Mn-oxide crust. Furthermore, muddy, carbonate-rich, yellow-brownish sediment was recovered (77GTV-1,2).

During station **78GTV** ultramafic rocks to the east of the Logatchev 1 field were sampled. The upper part of the grab sample consists of, up to 30 cm thick, Mn-crusts (group 78GTV-1; 30 samples, some with an Fe-oxide layer in the center). The Mn-layer shows several sublayers of shiny black, dense material with characteristic jointing (probably from rising diffuse hydrothermal fluids). The host rocks are serpentinized peridotites (in part with Mn-crusts; 78GTV-2,-5A,-5B), coarse grained websterites with cm-sized orthopyroxene and intergranular olivine (78GTV-3A,-3B), and distinctly weathered, coarse grained orthopyroxenites (78GTV-4A,-4B).

A full load of pelagic sediment overlying red to red-brown to orange Fe-oxyhydroxide-rich sediment was recovered during station **79GTV**. Few semi-lithified pieces are encrusted in Mn-oxyhydroxides that show atacamite deposition in cavities or as crusts.

Station **82GTV** aimed to sample in an area of a temperature anomaly, which was discovered during station 22-OFOS. Samples recovered include Fe-Mn-oxide crusts with irregular shape (82GTV1-1 to 8) and crusts of brownish material with intercalated Mn-Fe-layers and crusts (82GTV-2A1 to-4, -2B1 to -4). Ultramafics are greenish, dense pebbles mainly consisting of serpentine and talc (82GTV-3; 30 samples).

The objective of station **83GTV** was to sample the clam field at ANYA'S GARDEN, that was found during a previous ROV dive. Upon reaching the target, shells were located and sampled. The grab recovered a full load of sulfide-rich material with few empty shells of *Bathymodiolus*. The surface of the grabbed material consists of Fe-oxyhydroxides with some atacamite (83GTV-1). Few pieces of a former sulfide chimney (83GTV-5) were also recovered from the surface. They show concentric growth with a Fe-oxyhydroxide rim and relict sulfides in the core. This oxidized material is overlying silicified pyrite-rich crusts that are either cementing fragments of clay altered wall rock including cm-sized orthopyroxene crystals (83GTV-2) or occur as porous massive pyrite crust (83GTV-3). The crusts are underlain by secondary Cu-sulfides that form largely unconsolidated mud with few rounded fragments and cobbles of massive secondary Cu-sulfides (83GTV-4). Only one small piece of primary chalcopyrite was recovered (83GTV-6). The lower part of the grab sample consists of mud of presumably altered rock material (83GTV-8) containing two cobbles (up to 10 cm in diameter) of talc-bearing serpentinite (83GTV-7).

Significance: Similar to previous grabs (35GTV, 62GTV) this grab shows that large parts in the vicinity of IRINA II are covered by silicified cap rocks allowing for conductive cooling of the hydrothermal fluids and enriching the sulfides in a thin veneer underneath this crust.

The aim of station **87GTV** was sampling below a scarp south of the Logatchev 1 field. The most remarkable sample is a serpentinized peridotite/melanorite (87GTV-1) with a dense matrix and randomly oriented, cm-sized orthopyroxene crystals. The center of the sample contains a subrounded, 4 cm wide area, which could either be a xenolith or a somewhat less altered part of the rock. Strongly serpentinized dunite and websterite pebbles (group 87GTV-3) are regarded as part of the talus. One sample of fine- to medium grained gabbro-norite contained dark labradorite and golden orthopyroxene crystals (87GTV-2).

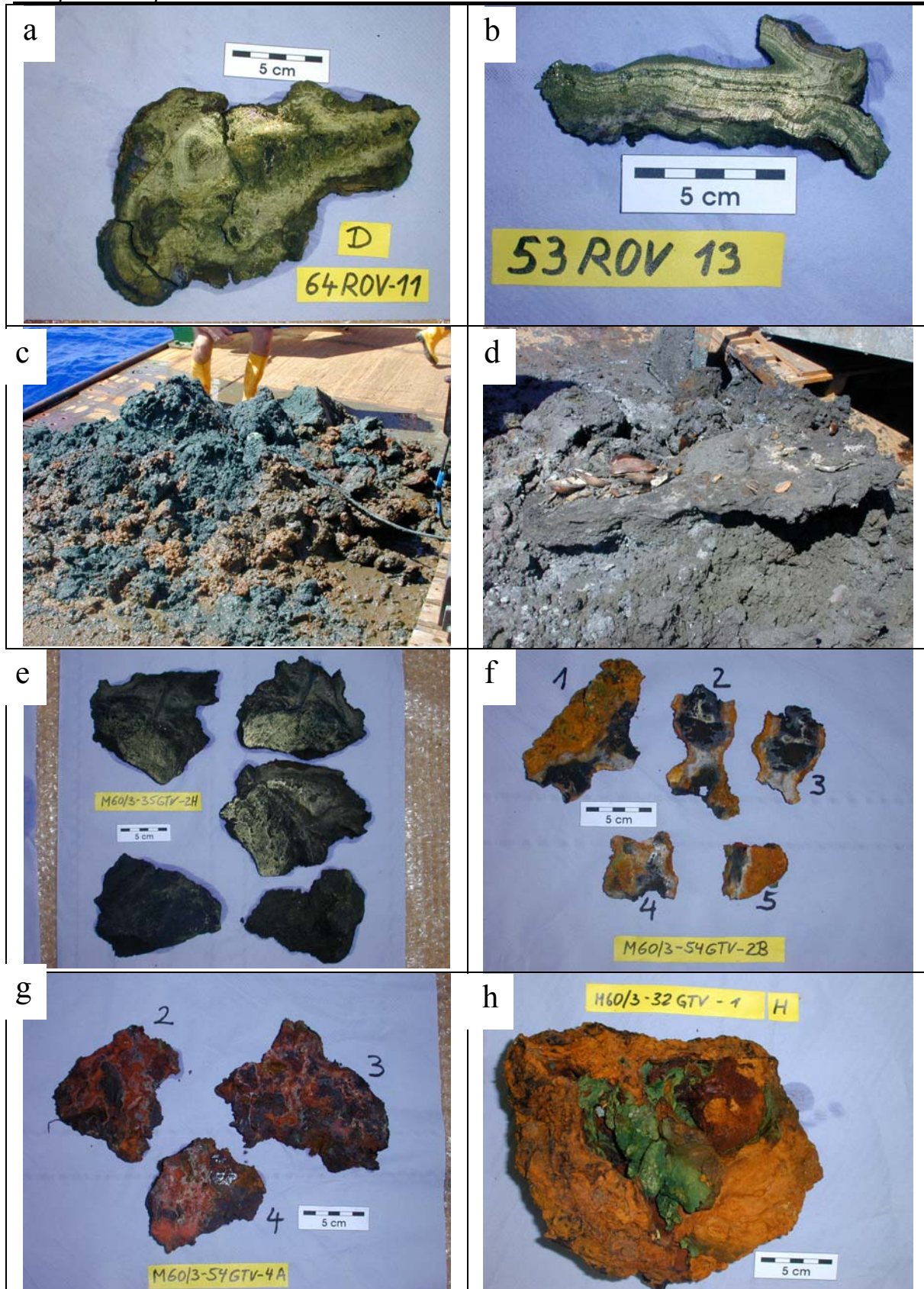


Fig. 3.17 Representative samples from the Logatchev 1 hydrothermal field. a,b) massive chalcopyrite chimney walls from black smokers. c) typical mud-rich sample from the periphery of the mound (32GTV). d) silicified crust acting as a cap rock (35GTV). e) massive chalcopyrite partly replaced by chalcocite and bornite. f) carbonate-quartz veins with native copper cutting secondary Cu-sulfides. g) hematite-rich breccias cementing chalcocite. h) Fe-oxyhydroxide crusts with abundant atacamite.

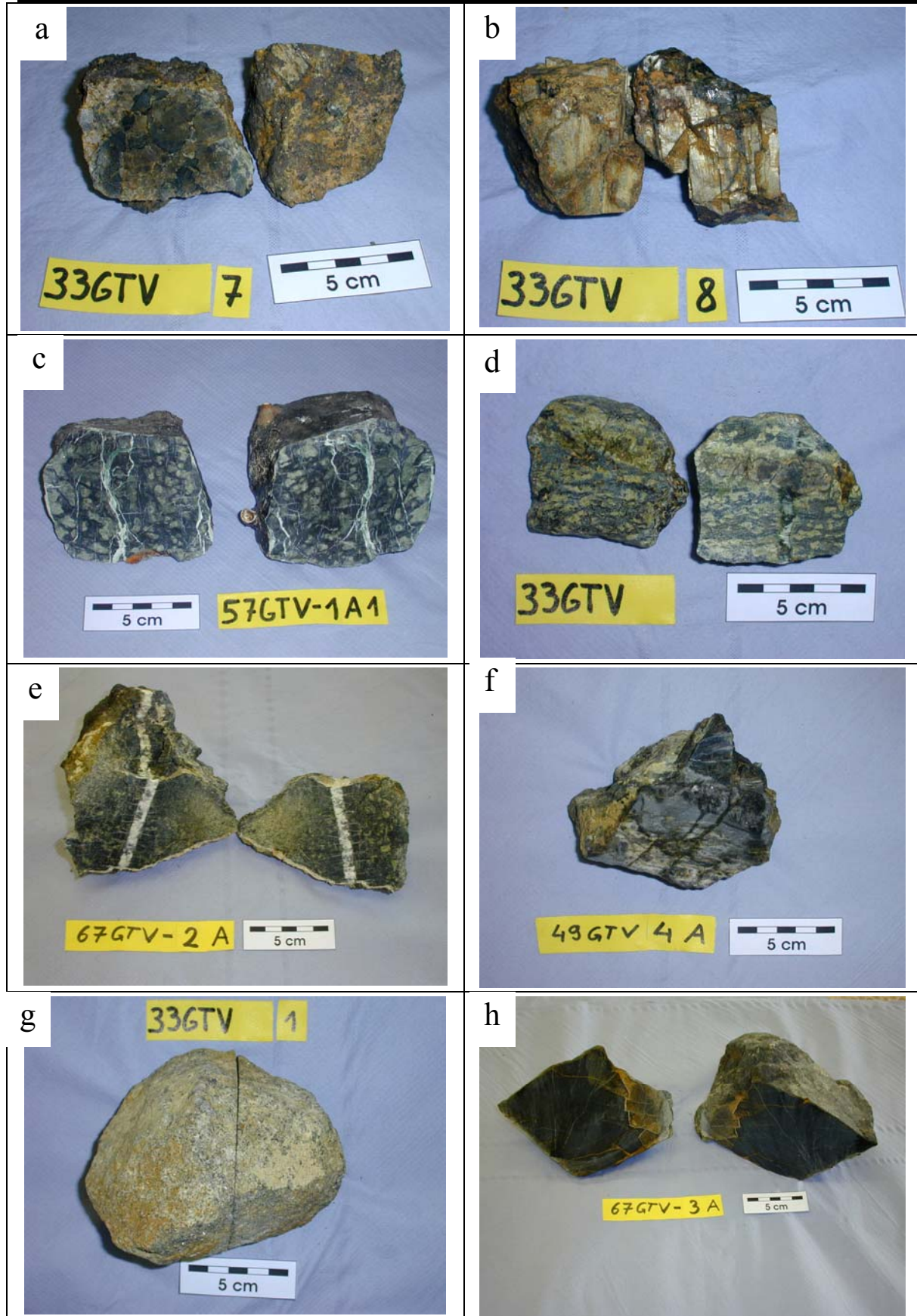


Fig. 3.18 Representative ultramafic samples from the Logatchev 1 hydrothermal field. a) websterite. b) fragment of an orthopyroxenite. c) altered dunite with serpentine vein. d) peridotite mylonite. e) serpentinite with talc/quartz vein. f) peridotite with silicic melt layers. g) gabbro-norite. h) basalt in contact with peridotite.

### 3.4.8 Gas chemistry

(R. Seifert, S. Ertl, J. Scholten)

#### 3.4.8.1 Introduction

After the discovery of hydrothermal venting systems in 1977 continued research on vent sites made obvious that hydrothermal circulation plays an important role in the evolution of the earth. Much attention has been focused on serpentinization processes because of their potential importance to early earth hydrothermal systems and because they generate significant amounts of H<sub>2</sub>, CH<sub>4</sub>, and possibly other organic compounds during mineral–fluid reactions. The Logachev field at 14°45'N on the MAR is the first hydrothermal field which was found on the top of completely serpentinized ultramafic rocks outcropping at the seafloor.

This study aims to elucidate the transformation of carbon species and reduced gases brought along by hydrothermal fluids taking into account the extent and relevance of hydrothermal cyclicity. For this purpose, samples of hydrothermal fluids and plumes of two areas along the MAR (Logachev and 4°-11°S) will be sampled during several expeditions and analysed for the concentrations and isotope signatures (C, H) of the main reactive gases methane and hydrogen as well as of other components of the carbon cycle namely C<sub>2</sub>-C<sub>5</sub> hydrocarbons, dissolved organic matter (DOC), CO<sub>2</sub>, and biomass. Reported are first results from the first cruise to the Logachev field.

#### 3.4.8.2 Samples and methods

For analyses of dissolved gases a total of 210 water samples were obtained from 17 CTD/Rosette and 7 ROV stations (Table 3.3).

*CTD data* were mostly recorded for the entire water column using a SEABIRD CTD Type 911 equipped with a rosette of 22 10L Niskin bottles. Water samples were taken during lifting keeping the sampler at a certain depth for a short time.

*Light dissolved hydrocarbons* were analysed on board applying a purge and trap technique (Seifert et al., 1991). The water sample is stripped by He and analyses in the outflowing gas stream are concentrated in cooled traps at -84°C. After degassing, the trapped gases are released to a gaschromatograph (CARLO ERBA GC 6000) equipped with a packed (activated Al<sub>2</sub>O<sub>3</sub>) stainless steel column and a flame ionisation detector (FID) to separate, detect and quantify individual components. Recording and calculation of results is performed using a PC operated integration system (BRUKER Chrom Star). Analytical procedures were calibrated daily with commercial gas standards (LINDE). Analyses were generally done within 12 hrs after sampling.

For on board *measurements of dissolved hydrogen* up to 615ml of sample is connected to a high grade vacuum in an ultrasonic bath and heated until boiling. Aliquots of the released gas are transferred via a septum from the degassing unit into the analytical system. A gaschromatograph (THERMO TRACE) equipped with a packed stainless steel column (Molecular sieve 5A, carrier gas: He) and a pulsed discharge detector (PDD) is used to separate, detect and quantify Hydrogen. Recording and calculation of results is performed using a PC operated integration system (THERMO CHROM CARD A/D). Analytical procedures were calibrated daily with commercial gas standard (LINDE).

Table 3.3: Sample list for CTD- and ROV stations.

Station	Long. N	Lat. W	No.	HC	H <sub>2</sub>	$\delta^{13}\text{C}_{\text{CH}_4}$	$\delta^2\text{H}_2$	He	$\delta^{13}\text{C}$ - DIC	$\delta^{13}\text{C}$ - DOC	<sup>222</sup> Rn
17 CTD	14°39,9	44°60,0	18	18	12						2
25 CTD	14°45,1	44°58,7	11	11	11	11		11	11	11	11
31 CTD	14°48,5	44°58,2	12	12	11						5
37 CTD	14°45,2	44°58,8	18	18	12	12					8
44 CTD	14° 54,1	44° 54,6	17	16	13	13		7			3
51 CTD	14°44,8	44°58,8	6	6	6	6	1				5
52 CTD	14°43,4	44°57,6	6	6	6	6		6	6		3
58 CTD	14°44,1	44°58,4	6	6	6	6		6			4
59 CTD	14°44,4	44°58,9	8	7	8	7		7			4
68 CTD	14°44,0	44°57,5	8	8	8	8		8			6
69 CTD	14°45,5	44°58,0	8	8	8	8		8			5
71 CTD	14°45,0	44°56,4	9	9	9	9					
75 CTD	14°44,8	44°59,1	10	10	10	10		10			7
76 CTD	14°44,5	44°59,3	9	9	9	9		9			6
81 CTD	14°42,4	44°54,5	10	10	10						
85 CTD	14°45,1	44°58,9	13	13	13	13		13			12
86 CTD	14°44,0	44°59,6	11	11	11	11		11			
23 ROV			3	3	3	3					3
38 ROV			5	5	5	4		1			2
53 ROV			6	6	5	5	4		5	3	4
56 ROV			3	3	3	3			2		3
64 ROV			5	5	5	5	2		5		3
66 ROV			3	3	3	3			3		3
73 ROV			5	5	5	5	3	1	5		5

HC = CH<sub>4</sub> and C<sub>2</sub>-C<sub>4</sub> hydrocarbons

For onshore measurements of the *He concentrations and isotopic signature*, water samples were taken immediately after finishing the respective station. The samples were sealed head space free and gastight in copper tubes. Measurements will be performed at the Universität Bremen, Fachbereich 1 (Tracer Oceanography).

Samples for the determination of  $\delta^{13}\text{C}$  of the dissolved light hydrocarbons were obtained by degassing the water samples with a vacuum - ultrasonic technique (see above). Aliquots of the released gas were transferred via a septum from the degassing unit into gastight glass ampoules filled with NaCl-saturated water for later on shore analysis by GC-Isotope-Ratio-Mass-Spectrometry.

For onshore analysis of *stable carbon isotopes of dissolved inorganic carbon (DIC)*, aliquots of unfiltered sample was spiked with NaOH and BaCl<sub>2</sub> directly after recovery to precipitate carbonate species. The analyses of  $\delta^{13}\text{C}$ -DIC will be made by Dual-Inlet-Isotope-Ratio Mass-Spectrometry (THERMO MAT 252).

For onshore analysis of *stable isotopes for dissolved hydrogen*, up to 10mL of gas obtained by vacuum/ultrasonic degassing of sample was frozen on molecular sieve 4A under liquid nitrogen in a pre-evacuated glass vial. The samples will be analysed via a molecular sieve 5A PLOT column and a GC-Isotope-Ratio-Mass-Spectrometer for  $\delta^2\text{H}$ -values.

Samples for radionuclide measurements were obtained by CTD and the ROV fluid sampling device. For  $^{222}\text{Rn}$  analysis water samples were filled into an extraction apparatus and a water-immiscible scintillation cocktail (MaxiLight) was added. The sample was shaken for 1.5 hours and the organic phase was transferred into a low diffusive LS-vial which was stored for isotope equilibration for three hours. Two liquid scintillation counters (Gurdian and Triathler) were available for on-board  $^{222}\text{Rn}$  measurements. Samples were counted for six hours. Final calibration of the procedure and calculations of specific activities will be performed in the home lab. A list of samples obtained during the cruise is given in Table 3.2. Additional water samples (up two litres) were taken for the determination of  $^{228}\text{Ra}$  and  $^{210}\text{Pb}$  from ROV stations 73 Rov, 66ROV, 53 ROV, 73ROV and 38 ROV.

### 3.4.8.3 Results

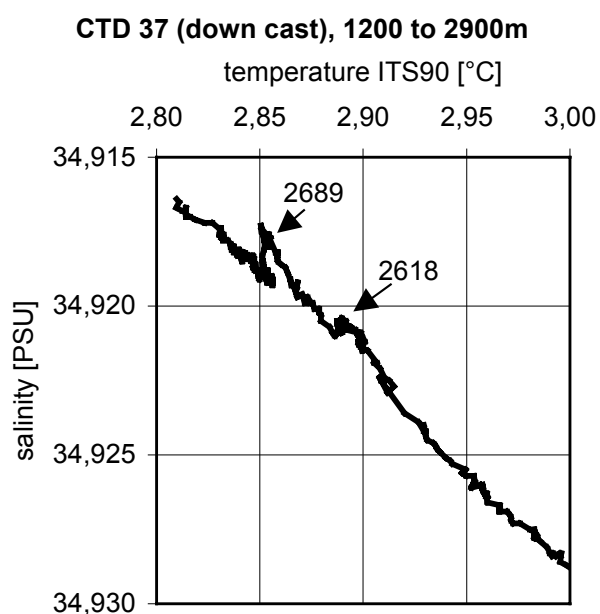


Fig 3.19 S/T diagram of deep waters, 37 CTD

dissolved gases and trace metals, this anomaly represents the hydrothermal plume of the Logatchev Field. However, such clear indications of hydrothermal influence did not appear in any of the other CTD profiles recorded. Therefore, on line information on the location of hydrothermal plumes within the water column for the selection of samples to be analysed for gases (hydrocarbons and hydrogen) and metal species was not available during most hydrocasts.

For most stations, no indication of hydrothermal plumes could be identified within the CTD-profiles. An exception is station 37-CTD for which the S/T plot evidences the intrusion of a component relatively depleted in salinity for the depth area from 2600m to 2700m water depth (Fig. 3.19). With regard to the data of

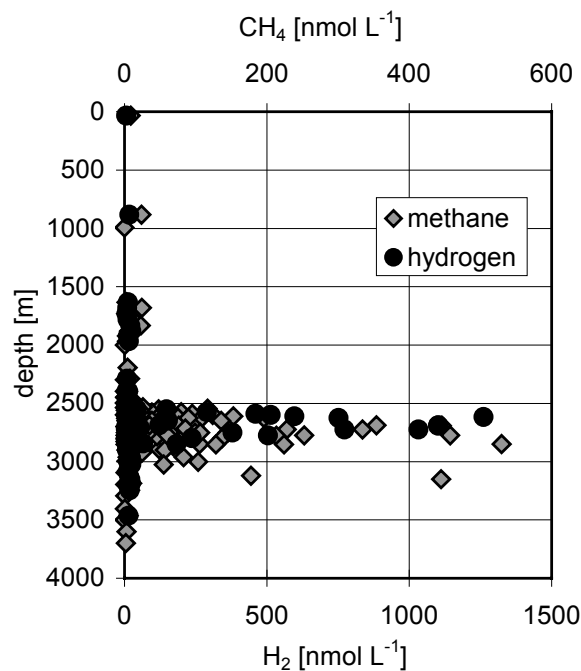


Fig. 3.20 Concentrations of  $\text{CH}_4$  and  $\text{H}_2$  in water samples of all CTD-stations

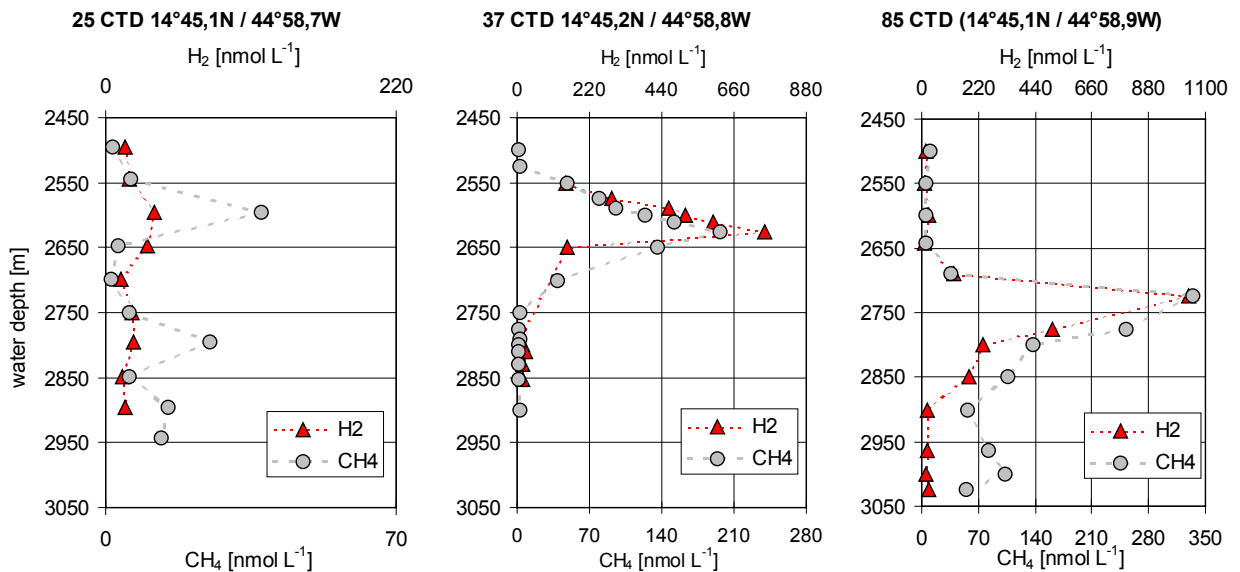


Fig. 3.21 Concentrations of  $\text{CH}_4$  and  $\text{H}_2$  in water samples of CTD-stations 25, 37, and 85.

Results for concentrations of dissolved methane and hydrogen obtained from CTD/rosette samples on board RV METEOR (Fig. 3.20) revealed a distribution of hydrothermal signatures over a wide zone of the water column covering the depth range from 2500m to 3000m water depth. Highest concentrations found are  $0.53$  and  $1.26 \mu\text{mol L}^{-1}$  for methane and hydrogen, respectively.

High  $\text{CH}_4$  concentrations correlate with high  $\text{H}_2$  concentrations in most cases. A considerable variety of the depths of maximum concentrations and of maximum  $\text{H}_2/\text{CH}_4$  ratios was observed. Figure 3.21 illustrates the results for 3 CTD stations carried out at the northern edge of Logatchev-1 field which are less than 0.2 nm apart.

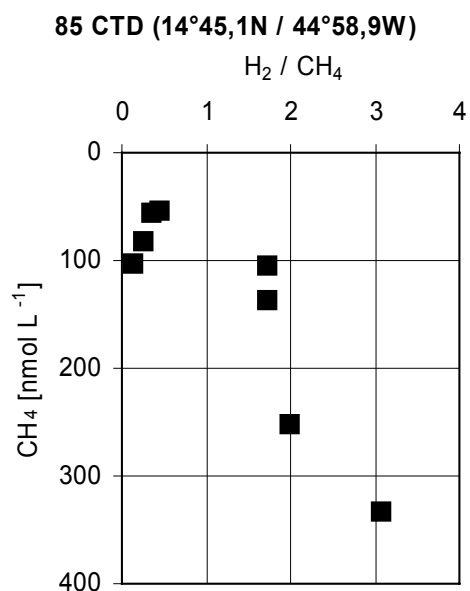


Fig. 3.22  $\text{H}_2/\text{CH}_4$  ratio vs.  $\text{CH}_4$  concentration for samples below 2700m water depth.

Two concentration maxima were present at station 25 at 2600m and 2800m water depth. (2600m:  $37.5 \text{ nmol L}^{-1} \text{ CH}_4$ ,  $36.4 \text{ nmol L}^{-1} \text{ H}_2$ ; 2800m:  $25 \text{ nmol L}^{-1} \text{ CH}_4$ ,  $21.5 \text{ nmol L}^{-1} \text{ H}_2$ ). Much higher concentrations were measured at stations 37 and 85. Station 37 revealed a distinct maximum at 2625m ( $196 \text{ nmol L}^{-1} \text{ CH}_4$ ,  $752 \text{ nmol L}^{-1} \text{ H}_2$ ); at station 85 highest concentrations occurred at 2725m ( $335 \text{ nmol L}^{-1} \text{ CH}_4$ ,  $1033 \text{ nmol L}^{-1} \text{ H}_2$ ) with strongly enhanced methane concentrations throughout the water column below. The  $\text{H}_2/\text{CH}_4$  ratio for these samples (Fig. 3.22) appears to decrease with decreasing methane concentrations hinting to an enhanced consumption rate for  $\text{H}_2$  compared to  $\text{CH}_4$ . This agrees with observations of Kadko et al. (1990) who found a very rapid removal of hydrogen from the plume compared to  $^{222}\text{Rn}$  decay and

methane oxidation for the Endeavour Ridge hydrothermal plume, but at much lower  $H_2$  concentrations of only up to  $12 \text{ nmol L}^{-1}$ .

Samples obtained by ROV directly at the hot fluid emanation sites revealed very high concentrations of dissolved hydrogen. Maximum concentrations found accounted for  $0.28 \text{ mmol L}^{-1}$  and  $1.8 \text{ mmol L}^{-1}$  of methane and hydrogen, respectively (Station 73 ROV). The resulting  $H_2/CH_4$  ratio of about 6.4 for this sample is in accordance with data reported by Charlou et al. (2002) for hydrothermal fluids of the Rainbow field that is also hosted in ultramafic rocks at the MAR. These authors give Mg-based calculated endmember concentrations of  $2.5 \text{ mmol L}^{-1}$  ( $CH_4$ ) and  $18 \text{ mmol L}^{-1}$  ( $H_2$ ), slightly above endmember gas concentrations estimated for Logachev with 12 and  $2.1 \text{ mmol L}^{-1}$  for  $H_2$  and  $CH_4$  respectively. In view of the good match of the  $H_2/CH_4$  ratios, one might assume our ROV sample to comprise about 10% of unaltered endmember fluid.

For hydrocarbons of carbon chain lengths from 2 to 4 only saturated homologues were observed (ethane, propane, butanes), but in low concentrations. Molar ratios between methane and higher homologues ( $C_1/C_{2-4}$ ) were generally above 2000.

### 3.4.9 Fluid chemistry

(A. Koschinsky, B. Alexander, L. de Carvalho, D. Garbe-Schönberg, U. Westernströer)

#### 3.4.9.1 Fluid sampling system for the MARUM ROV QUEST

For the direct sampling of hydrothermal fluids from high temperature vents a pumped flow-through system (Kiel Pumping System, KIPS) was used. The system was newly constructed and is entirely made of inert materials (Teflon, titanium). Samples are collected via a titanium tube of 100 cm length which can be directly inserted into the hot vent orifice. PFA tubing connects this sampling probe to 7 parallel PFA Teflon sampling flasks (490 ml Volume each, "Bottle #1" to "Bottle #7") and a standard deep sea impeller pump (SeaBird, U.S.A.) mounted downstream to the sampling flasks (Fig. 3.23). Each sampling flask has linked open-close valves (valve set #1 to #7) with handles which are operated by the ROV's manipulator (Figs. 3.23, 3.24). The sampling flasks are mounted with a few degrees inclination and equipped with all-Teflon overpressure valves. Eventually released gases and fluids can be collected in gas-tight bags fitted to the valves. In-line PFA Teflon filter holders in front of each sampling flask allow *in-situ* filtration of sampled fluids. An additional open-close valve set (valve #8) bypasses the sampling flasks and was used as a sampling line for microbiology *in-situ* filtration. The whole system is contained within a plastic frame mounted on the ROV's tools sled. For sub-sampling the whole system was removed from the ROV and transferred to the laboratory. Two sample flasks were filled at every sampling location (Bottles #2 and #7, #3 and #6, #4 and #5). This accomplishes the study of fluid chemistry and dissolved gases on sub-samples that are as identical as possible.

### 3.4.9.2 Fluid sampling and filtration

Three bottles from the KIPS fluid sampling system (bottle #2, #3, #4) and all three Niskin flasks (N1, N2, N3) mounted on the ROV were sub-sampled in the laboratory immediately after recovery of the ROV. The fluid samples were pressure-filtrated with Argon (99.999%) at 0.5 bar through pre-cleaned 0.2  $\mu\text{m}$  Nuclepore PC membrane filters by means of polycarbonate filtration units (Sartorius, Germany). The filtrates were separated into aliquots for voltammetric and ICP analyses and acidified to pH 1 with 100  $\mu\text{l}$  subboiled concentrated nitric acid per 50 ml (ICP) and with suprapure HCl to pH 2 (voltammetry), respectively. Procedural blanks were processed in regular intervals. All work was done in a class 100 clean bench (Slee, Germany) using only all-plastic labware (polypropylene, polycarbonate, PFA-teflon). Rinse water was ultrapure ( $>18.2$  Mohm) dispensed from a Millipore Milli-Q system.

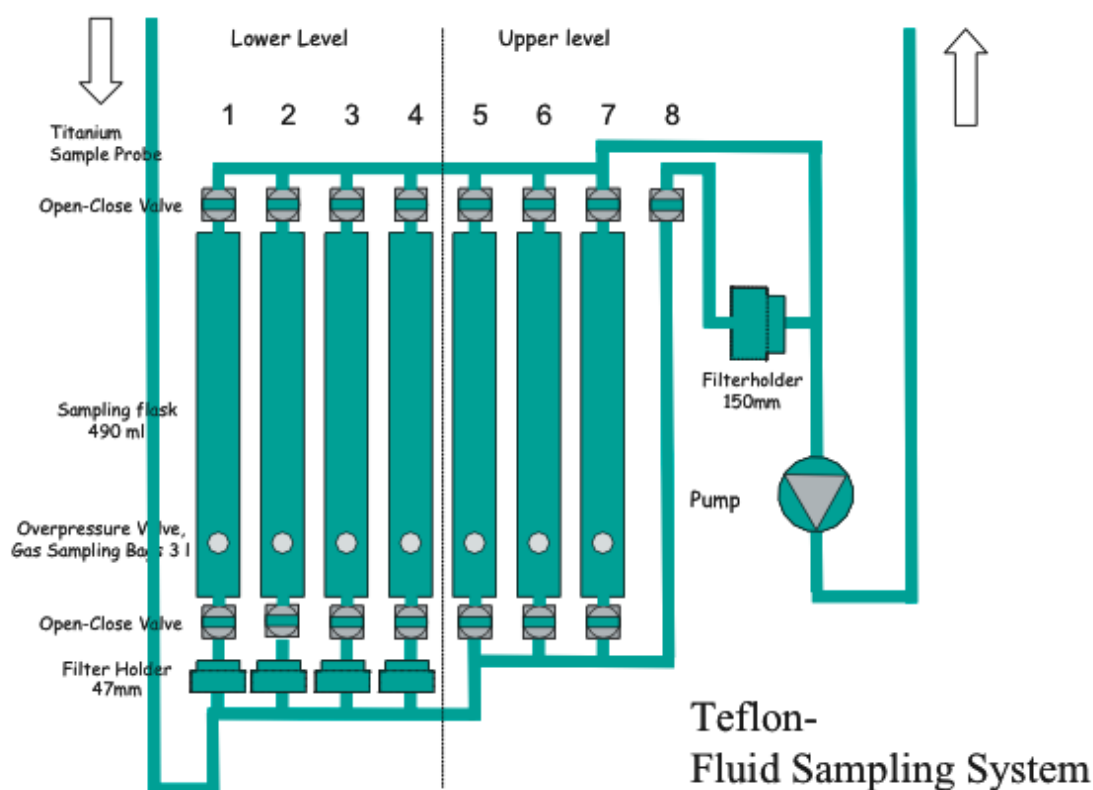


Fig. 3.23: Schematic drawing of the Kiel fluid sampling system for in-situ sampling of hydrothermal vent fluids.

A total of 34 bottle samples from the fluid sampling system, and 20 Niskin samples were taken (Table 3.4). After return to the home labs, in Kiel selected samples will be analysed for major (Mg, Ca, Ba, Sr, Na, K, Si, Fe, Mn, B, Cl) and trace element composition (e.g., I, Br, Li, Al, Cs, Ba, Sr, Y-REE, Fe, Mn, Cr, V, Cu, Co, Ni, Pb, U, Mo, As, Sb, W, PGE) by ICP-OES (Spectro Ciros SOP CCD) and ICP-MS using both collision-cell quadrupole (Agilent 7500cs) and high-resolution sector-field based instrumentation (Micromass PlasmaTrace2). At IUB in Bremen, voltammetry will be used for further trace metal analyses (Zn, Cd, Pb, Cu, Co, Ni, Ti, V, Mo, U, Tl, Pt). Li and Na will be analysed by flame photometry, and an autoanalyzer will be used to determine anionic compounds (silicate, phosphate, nitrate,

sulfate, chloride) and dissolved organic carbon DOC. The duplicate coverage of some elements with different methods will be used for the evaluation of the methods and the data.

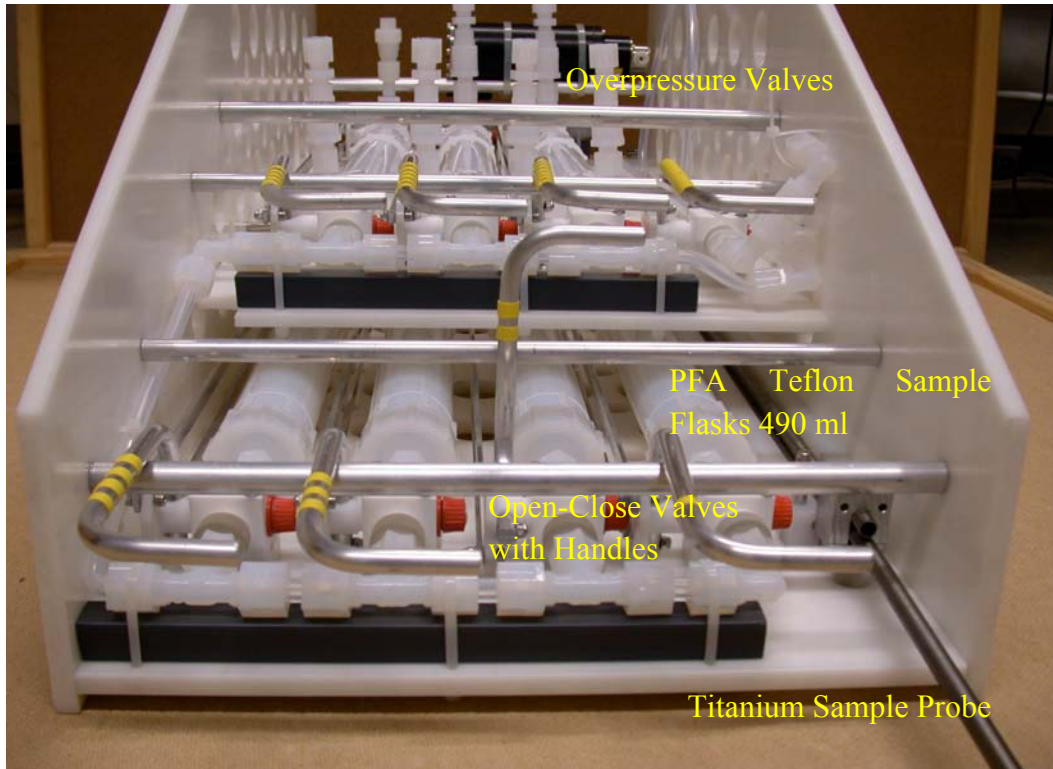


Fig. 3.24: Front view of the Kiel fluid sampling system showing the titanium sample probe (right), valve handles, PFA Teflon sampling flasks, and overpressure valves (top).

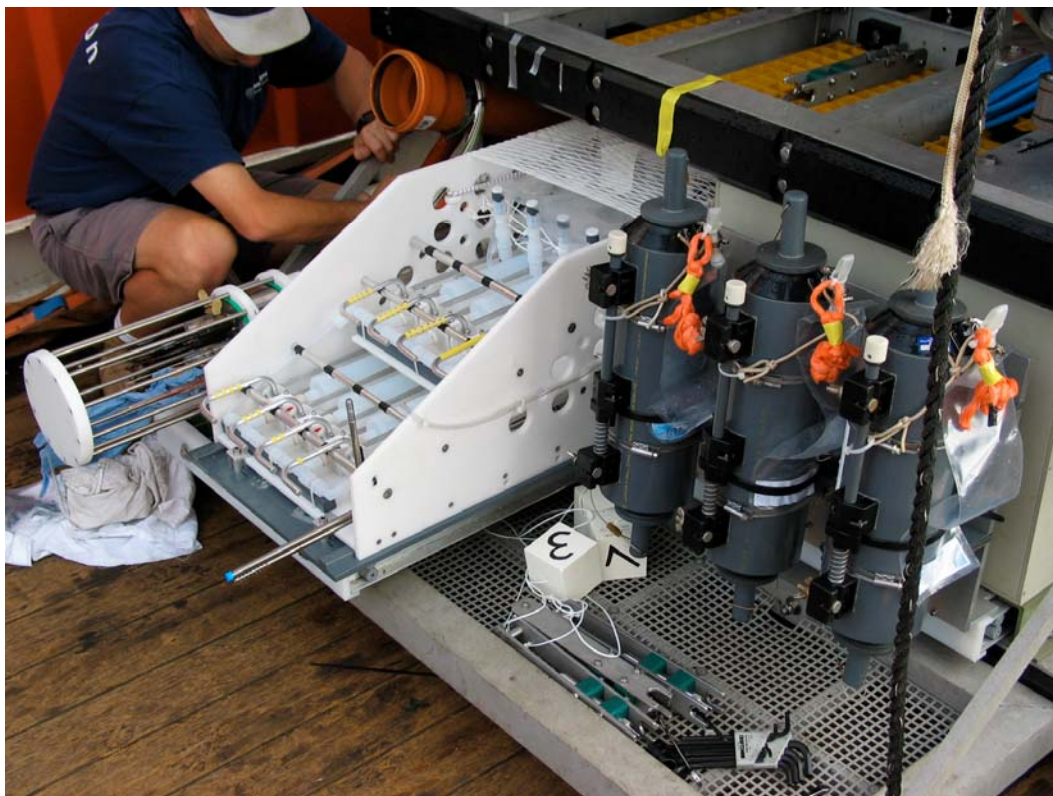


Fig. 3.25: The fluid sampling system mounted on the tools sled of the Bremen MARUM ROV QUEST besides Niskin bottles and the MPI Bremen sensor array.

Table 3.4: Samples for Trace Element Geochemistry

St. No	Instrument	Dive type	Location	Lat (N)	Long (W)	Water depth (m)	B	B	B	B	B	B	B	B	N	N	N
M 60/3							1	2	3	4	5	6	7	8	1	2	3
23	ROV	Geo	IRINA II	14° 45,196	44° 58,787	3044			TM	TM	G		G	MB			G
29	ROV	Geo	IRINA	14° 45,111	44° 58,710	2976		TM			G	G	TM	MB	TM	TM	
													G		G	G	
38	ROV	Bio	IRINA II	14° 45,185	44° 58,750	3031	S	TM	TM	TM	G	G	G	MB	TM	TM	TM
53	ROV	Geo	IRINA	14° 45,084	44° 58,709	2959	S	TM	TM	TM	G	G	G		TM	TM	TM
															G	G	G
56	ROV	Bio	IRINA II	14° 45,217	44° 58,814	3041		TM				G	G	MB		TM	TM
																G	
64	ROV	Geo	Anna-Louise	14° 45,070	44° 58,690	2948		TM	TM			G	G		G	TM	TM
																G	G
66	ROV	Bio	IRINA & IRINA II	14° 45,083	44° 58,696	2959	TM	G	TM			G			TM	TM	TM
																	G
73	ROV	Geo	IRINA II	14° 45,206	44° 58,741	3033	S	TM	TM	TM	G	G	G		TM	TM	TM
															G	G	

TM: Trace metals and speciation chemistry; G: Gas chemistry; MB: Microbiology; S: Sulfur isotopes and organic complexation; B: Sampling-Bottle from KIPS fluid sampling system; N: Niskin-Bottle. Bottle pairs (TM/S-Analytics and Gas chemistry): B2 - B7, B3 - B6, B4 - B5.

### 3.4.9.3 Onboard measurements: pH and Eh measurements, sample preparation and chloride titration

The fluid samples were obtained from the fluid sampling system coupled to the ROV QUEST and from the CTD/Rosette water sampler. Especially the anoxic fluids from the hot vents were analyzed and stored immediately after system recovery. Filtered and non-filtered samples (partly acidified to pH 2 with suprapure HCl) were subjected to immediate voltammetric speciation analysis (see below). Parallel to that, pH and Eh measurements (Mettler electrodes with Ag/AgCl reference electrode) were carried out in unfiltered sample aliquots. All fluid samples were stored in a refrigerator at 4°C between the analyses. To identify a possible influence of phase separation, all vent fluid samples and some samples from the water column profiles were analysed for chloride by titration with AgNO<sub>3</sub> after the method of Fajans, using fluoresceine-sodium as indicator. From selected samples, about 150 ml of fluid were filled into specially precleaned bottles and immediately deep-frozen at –20°C. These samples were shipped in frozen state for the determination of organic metal complexation in the home laboratory of the project partner Dr. Sylvia Sander (University of Otago, New Zealand).

### 3.4.9.4 Onboard measurements: Voltammetric analyses of trace metal speciations and concentrations

For onboard speciation and trace metal concentration analyses, the electrochemical method of voltammetry was used. Voltammetry is able to differentiate between different redox species and (in combination with UV digestion of the water samples) free and complexed forms of ions in solution and is highly sensitive. All voltammetric measurements were performed using two Metrohm equipments: a 693 VA Processor in combination with a 694 VA Stand (all from Metrohm, Herisau, Switzerland), and a 757 VA Computrace run with a standard PC. The three-electrode configuration consisted of the hanging mercury droplet electrode (HMDE) as the working electrode, an Ag/AgCl reference electrode (3 mol l<sup>-1</sup> KCl), and a platinum wire as the auxiliary electrode.

Immediately after recovery, the fluid samples were prepared for speciation analyses onboard. The unfiltered samples were used for determination of the total content of the metals, while filtered (0.2 µm) samples were prepared for determination of the total dissolved content of the metals. Both the filtered and unfiltered samples were submitted to a digestion process in a UV Digester (Model 705, Metrohm), which contains a high pressure mercury lamp (500 W). After 2 hours UV irradiation, the total content (filtered and non-filtered) of iron, chromium and arsenic in the samples were determined by the standard addition method ( $n = 3$ ).

Before the voltammetric determination of the total content of the metals in the digested samples, the redox speciation of Fe, Cr and As was carried out. Firstly, the concentrations of active Fe (non-filtered), Fe(II) and Fe(III) were determined in the undigested samples using the cathodic stripping voltammetric method developed by van den Berg (Aldrich and van den Berg, 1998). In this method, Fe(III) is determined with 1-nitroso-2-naphthol as complexing reagent and catalytic reaction with bromate, masking of Fe(II) with Bipyridyl. Fe(II) is determined by subtraction of Fe(III) from total Fe. Total and total dissolved iron are

determined after UV digestion as iron(III) but without addition of Bipyridyl. After the determination of the iron redox species, the determination of the arsenic speciation was carried out in the undigested samples by cathodic stripping voltammetry (Barra and dos Santos, 2001). In this method, As(III) is determined in a 1 M HCl and 10 mg/L Cu(II) supporting electrolyte. As arsenate is electrochemically inactive at the mercury electrode, total As is determined after the UV digestion using the rotating gold electrode (Au-RDE; Application Bulletin Metrohm 226/2). As(V) is calculated by subtraction of As(III) from total arsenic. After evaluating of the iron and arsenic concentrations in the fluid samples, the chromium redox speciation was carried out in the undigested samples by the catalytic cathodic stripping voltammetric method developed by van den Berg (Boussemart et al., 1992) and adapted to hydrothermal fluid samples by Sander and Koschinsky (2000). This method uses diethylenetriaminepentaacetic acid (DTPA) as the complexing reagent for Cr(VI) and catalytic reaction with nitrate. Firstly, the concentration of reactive total Cr is determined by addition of DTPA to the sample just before the voltammetric measurement. For the

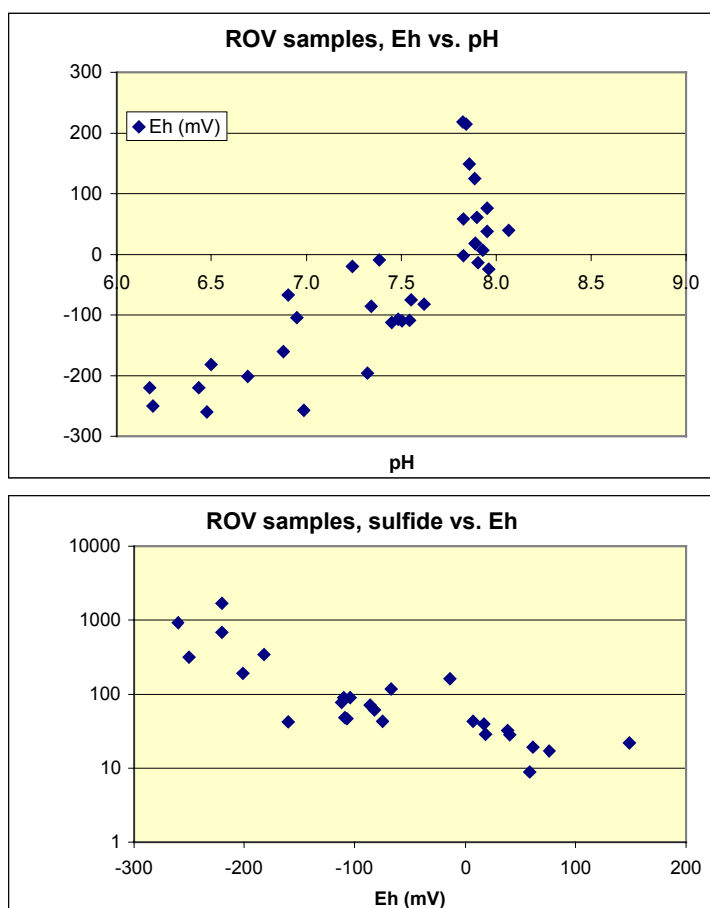


**Fig. 3.26:** Correlation of pH, Eh and sulfide concentrations in the ROV fluid samples

determination of Cr(VI), DTPA is added to the samples and the voltammetric measurement is carried out after 30 min. The concentration of reactive Cr(III) is obtained by subtraction of reactive total Cr from Cr(VI). The total and total dissolved Cr concentrations are determined after the UV digestion. The concentration of dissolved total Cr(III) is obtained by subtraction of total dissolved Cr from Cr(VI).

The analysis of S, Se, Mn, Cu, Pb, Cd, and Zn on ROV samples was sequential, and generally proceeded in the following order: 1) non-filtered, non-digested samples, 2) filtered, non-digested samples, 3) non-filtered and filtered digested samples. Following removal of samples from the ROV fluid sampling system,

unfiltered samples were immediately analyzed for sulfide ( $S^{2-}$ ) in a nitrogen purged 0.6 M NaCl solution using a polarographic method (Luther III et al., 1985). Following sulfide analysis, polarography (Madureira et al., 1997) was used to concurrently determine sulfate ( $SO_4^{2-}$ ) and thiosulfate ( $S_2O_3^{2-}$ ) concentrations in the non-filtered samples. Sulfur species concentrations were determined for only non-filtered, non-digested samples. Concentrations

of Se(IV) in non-digested samples was determined by anodic stripping voltammetry (ASV) with 10 mg/L Cu(II) and 0.025 M HCl as supporting electrolyte (van den Berg and Khan, 1990). Total Se was measured in digested samples, and Se(VI) calculated as the difference between total Se and Se(IV) measured in non-digested samples. Due to insufficient method detection limits, samples collected during ROV deployments subsequent to the 38ROV station were not analyzed for Se. Manganese concentrations were determined using ASV (Application Bulletin Metrohm 123/3) with 0.1 M sodium tetraborate as supporting electrolyte. For Cu, Pb, Cd, and Zn analyses samples were buffered at pH 4.6 with 1 M acetate before measurement by ASV (Application Bulletin Metrohm 231/2). The quantification of S, Se, Mn, Cu, Pb, Cd, and Zn in the samples was performed by the standard addition method ( $n = 3$ ).

### 3.4.9.5 First results of the onboard analyses

#### ROV vent fluid samples

First of all it must be noted that all hydrothermal fluid samples were diluted by seawater and the results presented here are not yet recalculated to endmember compositions. The pH and Eh measurements in the samples taken directly from the vent sites with ROV clearly reflect the contribution of hot reducing hydrothermal endmember fluid and oxic seawater, respectively. The plot of Eh versus pH (Fig. 3.26) indicates only slightly depleted pH values (minimum 6.2) compared to the background value of 7.9. The most undiluted fluids show significantly reduced Eh potentials, which correlate with the contents of sulfide (Fig. 3.26). However, in contrast to fluids from many other hydrothermal fields, sulfide concentrations were found to be quite low (maximum 0.05 mM were measured) compared to the extremely high concentrations of methane and hydrogen (see chapter 3.4.7). This is interpreted as a typical feature of fluids influenced by serpentinization reactions.

The variability of Cl concentrations measured in the fluid samples is in the range of 4 % only, indicating that all samples have chlorinities very similar to ambient seawater. A slight tendency towards decreased salinities seems to be visible in Fig. 3.27 in which chloride was

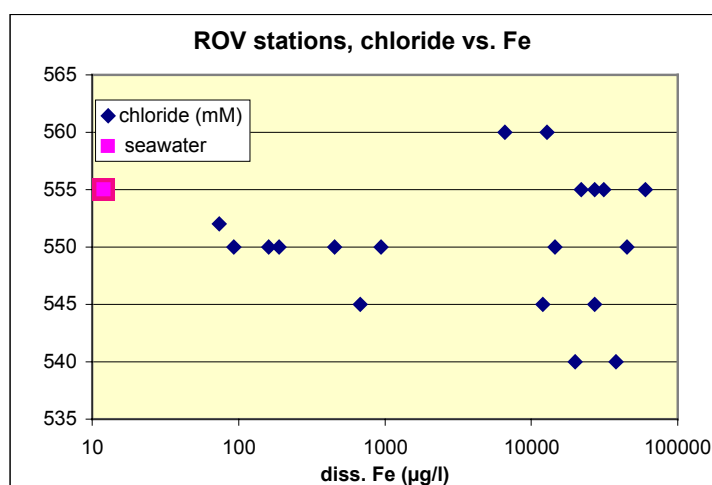


**Fig. 3.27:** Variability of chloride concentrations in relation to dissolved Fe concentrations

plotted against Fe as hydrothermal element. This would be consistent with a vapor-like fluid deriving from supercritical (>400°C, >300 bar) condensation, however, the range of the decrease is close to the range of the analytical precision (2 %).

With respect to the speciation analyses, the Fe data provided the most interesting results while Se data were mostly below the detection limit of 2.5 nM. Also most data for

Cr and As species showed that these compounds were not enriched to a significant degree in the fluids, but were probably mostly bound in particulate phases, as some increased concentrations in non-filtered samples indicated. Also intermediate sulfur species (sulfite, thiosulfate) were found only at low concentrations in a few samples. Fe was the dominating heavy metal in all fluid samples, with a certain particulate contribution in the form of Fe sulfides. The speciation distribution graph (Fig. 3.28) demonstrates the dominance of Fe(II) over Fe(III) and shows that about 90 % of the total Fe are present in a free reactive form. Obviously, the Fe speciation can differ in different samples, for example 64ROV shows the highest Fe(II)/Fe(III) ratio of all samples, although the total Fe concentration (0.45 mM) is lower than that of 53ROV (3.8 mM).

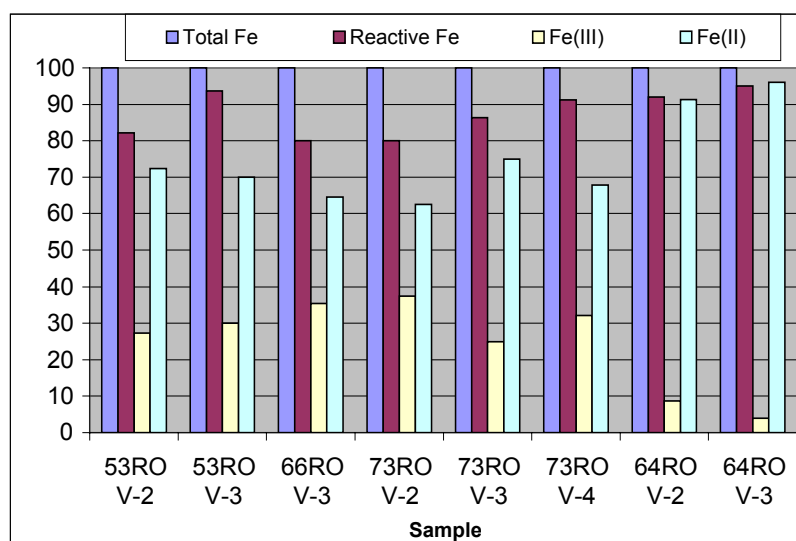


Fig. 3.28 Fe speciation in different ROV fluid samples

The second most enriched metal was Mn with maximum concentrations of 45 mM, followed by Cu (max. 27 mM total Cu) and Zn (max. 13 mM). Much of the Cu was found to be bound in particulate phases, while free dissolved Cu was found to be much lower with max. 1.5 mM. Pb (up to 0.09 mM) and Cd (mostly <0.005 mM) were comparatively

low. The high Fe/Mn and Fe/Cu ratios in our M60/3 fluid samples compared to fluid data reported by Douville et al. (2001) for different MAR vent systems indicate a close similarity to the Rainbow hydrothermal field and a pronounced influence of serpentinization reactions compared to purely basaltic systems.

All data reported here are measured values and have to be extrapolated to endmember concentrations using Mg concentrations (hydrothermal endmember Mg = 0, seawater endmember Mg = 55 mM).

### Water column profiles

In the samples taken by the CTD/rosette water sampler in vertical profiles in the water column, only pH and Eh measurements were carried out routinely, while for all other parameters, the hydrothermal signals were mostly too dilute to be detected. Eh measurements could be shown to be a good indicator for the hydrothermal plume because in profiles with pronounced methane and hydrogen maxima (see chapter 3.4.8), a good correlation of these maxima with decreased Eh values could be found (Fig. 3.29). This plume peak could also be identified by Fe measurements (Fig. 3.29).

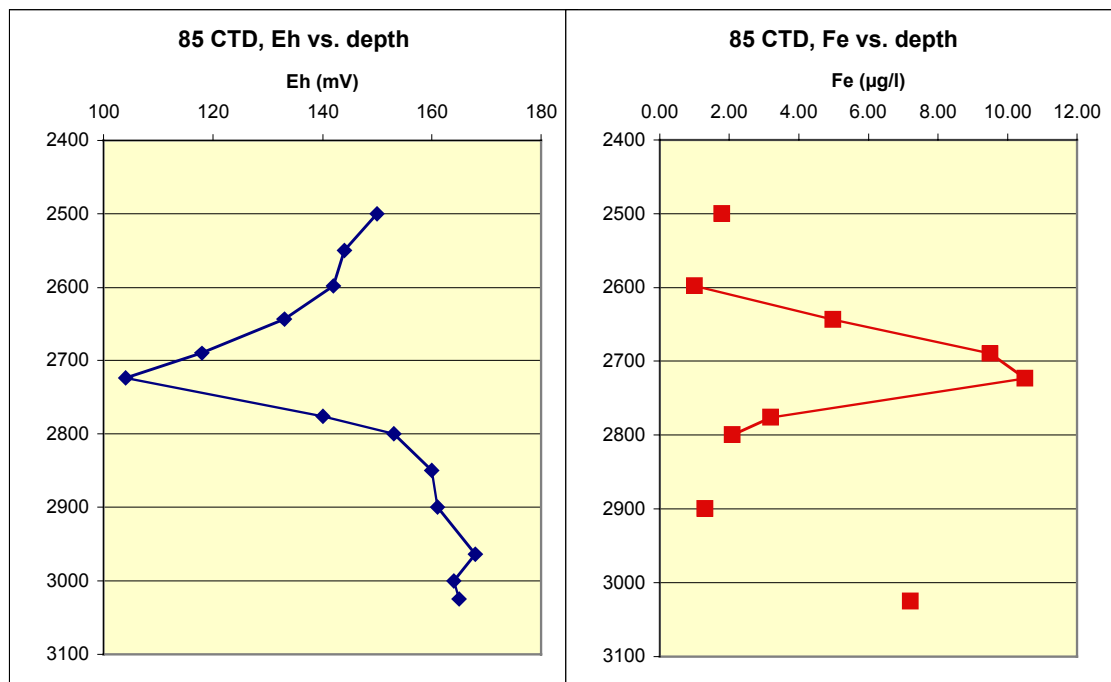


**Fig. 3.29:** Depth profiles for Eh and Fe at station 85 CTD, indicating a pronounced hydrothermal plume peak at about 2700 m depth

### 3.4.10 Hydrothermal symbioses

(C. Borowski, F. Zielinsky)

The biomass in the Logatchev vent field is primarily produced by the mussel *Bathymodiolus* aff. *puteoserpentis* (Gebruk et al. 2000) which lives in dual symbiosis with sulfide- and methane-oxidizing bacteria (Distel et al. 1995). This species was found during the M60/3 in dense aggregations around the IRINA II site. There was a large mussel bed with a diameter of more than 30 m along the southwestern slope of the chimney complex of the IRINA II mound and the vertical walls of the central sulfide complex were densely populated (mussel beds also occurred in the north and northwest of the chimney complex). Other symbiotic invertebrates encountered during M60/3 were shrimp of the genus *Rimicaris* which were densely aggregated on the IRINA II sulfide complex, and a population of thyasirid clams which we found buried in sediments near the marker "ANYA". We did not rediscover the population of vesicomid clams reported from ANYA'S GARDEN by Gebruk et al. (2000), but instead observed an aggregation of empty vesicomid clam shells in the vicinity of marker "Anya".

The major purpose of the symbiosis project was to sample, dissect, and preserve *Bathymodiolus* specimens from different microhabitats in order to investigate the relationship between the activity patterns of their thiotrophic and methanotrophic symbionts and the availability of their respective electron donors H<sub>2</sub>S and methane. Further issues were to sample shrimp and clams for the phylogenetic and functional characterisation of their symbionts, mussels for analyses of trace metal accumulation in co-operation with the IUB fluid-geochemistry group. All analyses will be done at the MPI-Bremen and associated laboratories.

Different types of microhabitats of *Bathymodiolus* were identified during the ROV dives by video observation and in-situ temperature measurements with the “PROFILUR” sensor system (Chapter 3.4.4). *Bathymodiolus* specimens were scratched off specific microhabitat substrates with stalked scratch nets (20 cm diameter opening) operated by the seven-function manipulator arm of the ROV, and the filled nets were stored in the ROV sample storage box (Fig 3.30). At selected animal collection sites, additional water samples were collected for analysis of methane concentrations and  $\delta^{13}\text{C}$  composition, as well as sulfide and trace metals concentrations to gain a more detailed characterization of the animals' geochemical environment. These samples were obtained with Niskin water samplers which were mounted to the front of the ROV tool sled, and individually tripped by the ROV manipulator arm. Analyses of the water samples were performed on board or will be done in the home-based laboratories of the IfBM biogeochemistry and the IUB fluid geochemistry groups. A considerable number of *Bathymodiolus* specimens was also recovered from the IRINA II mussel bed with 35 GTV. While these specimens were used for trace metal analyses, they were not useful for molecular and morphological analyses because the high temperatures of the substratum that they were attached to ( $>100^\circ\text{C}$  measured in only 10 – 15 cm depth bsf) cooked the animals when the overlying water drained off as the grab was lifted from the water onto the ship. Thyasirid clams were collected by dredging with the scratch net in surface sediments. Shrimp were suctioned from their habitat with the slurp gun (Fig. 3.31) and transferred to a modified baited trap that was installed in the ROV sample storage box stored where they were kept during the rest of the dive.

Table 3.5: Specifics for ROV samples used for hydrothermal symbiosis research.

Sample no.	Location	Sample type	Time, UTC	ROV Position	PROFILUR temp. peak/aver., °C	Target organisms
38 ROV /4	Mussle bed near marker “IRINA II”	Scratch net	16:06	14°45.1842' N 44°58.7477' W	5.5 / 3.75	Mussels
38 ROV /6	Top of sulfide pillar next to IRINA II main structure	Scratch net	17:00	14°45.1878' N 44°58.7469' W	3.9 / 2.75	Mussels
56 ROV /6	Vertical wall of IRINA II main sulfide structure	Scratch net	22:07	14°45.1892' N 44°58.7374' W	2.76 / 2.7	Mussels
56 ROV /5	Vertical wall of IRINA II main sulfide structure	Slurp gun	21:47	14°45.1890' N 44°58.7372' W	3.6. / 2.7	Shrimp
66 ROV /13	Sediments near Marker “Anya”	Scratch net	19:19	14°45.2170' N 44°58.8133' W	2.7 / 2.7	Thyasirid clams
66 ROV /16	IRINA II mussel bed, downhill margin	Scratch net	20:20	14°45.1887' N 44°58.7399' W	3.0 / 2.8	Mussels

After recovery of the ROV, the animals were stored in chilled sea water and dissected as soon as possible for the various analytical purposes. The gills, foot tissues, and digestive glands of *Bathymodiolus* specimens were dissected and fixed for molecular biological analyses of 16S ribosomal RNA (rRNA) and messenger RNA (mRNA), fluorescence in situ hybridization (FISH), stable isotope analyses, trace metals and microbial biomarkers, and for

transmission electron microscopy (TEM). Tissues of the thyasirids were dissected as the mussels and preserved for analyses of 16S rRNA, FISH, and TEM. From the shrimp, the symbiont bearing maxillipeds were dissected and preserved for similar analyses.

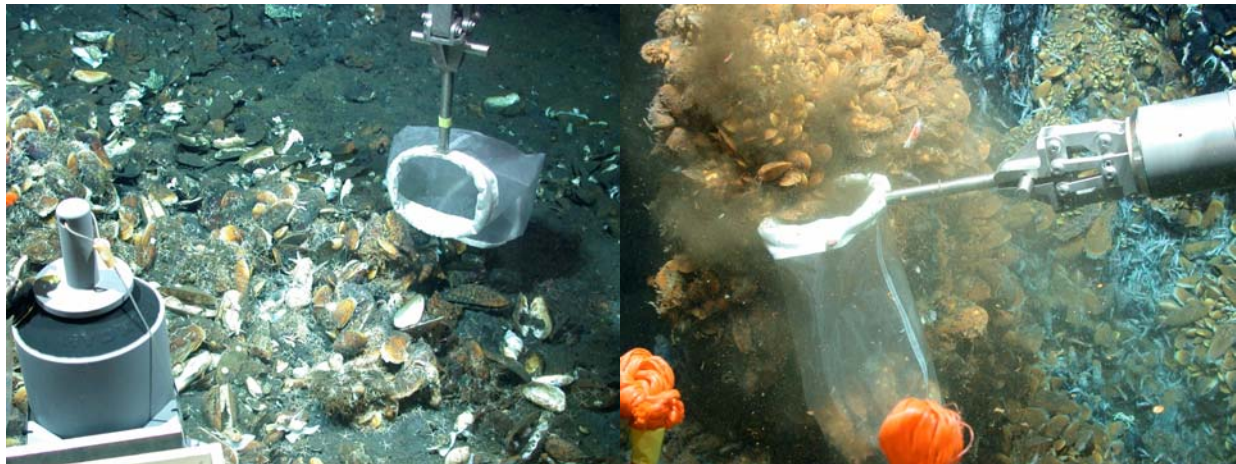


Fig. 3.30 Sampling of two different microhabitats of *Bathymodiolus* aff. *puteoserpentis*. Left: Sample 38 ROV /4 near marker IRINA II in the mussel bed; note the Niskin water sampler mounted to the ROV tool sled which is already closed. Right: sample location 38 ROV /6 on a sulfide pillar.



Fig. 3.31 Left: Dense aggregations of *Rimicaris* shrimp on the walls of the central sulfide structure of IRINA II. Right: Slurp gun sample of *Rimicaris*.

### 3.4.11 Marine microbiology

(J. Imhoff, J. Süling, J. Küver)

#### 3.4.11.1 Introduction

Microbial life is abundant at hydrothermal vent ecosystems and is expected to span the whole temperature range that enables life and reproduction of microbial cells. Though quite a number of studies have been made at hydrothermal vent sites world wide, little information is available on the phylogenetic and metabolic diversity of microorganisms along physical and chemical gradients of hydrothermal vents. Parameter like temperature, availability of oxygen and electron donors and mineral salts composition of the hydrothermal fluids are considered

as major factors controlling microbial life in general and species distribution in particular. Due to the abundance of reduced sulfur compounds such as sulfide, sulfite, thiosulfate and tetrathionate, microorganisms depending on the turnover of sulfur compounds are abundant in hydrothermal vent habitats. Both autotrophic as well as heterotrophic sulfur oxidising bacteria apparently are abundant (Teske et al., 2000; Podgorsek et al., 2004). In recent years, Epsilonproteobacteria, many of which are known to reduce and oxidise elemental sulfur, were found to be abundant at hydrothermal vent sites. Their ecological function in hydrothermal vent ecosystems, however, is not well understood (Campbell et al., 2001; Reysenbach et al., 2000; Corre et al., 2001).

### 3.4.11.2 Main objectives

The main objectives during the METEOR M 60/3 cruise were:

- Identification of important functional microbial groups and their most prominent members.
- Determination of colonization structure, diversity and activity of bacteria and archaea and their change under the influence of the properties of hydrothermal fluids.
- Influence of physical and chemical factors on the succession of microbial communities in hydrothermal gradients.
- Determination of physiological groups of microorganisms in defined ecological niches.
- Enrichment and isolation of microorganisms adapted to hydrothermal vent ecosystems.

### 3.4.11.3 Sampling and experiments

In order to describe microbial communities of hydrothermal vent ecosystems and their mutual interdependencies on physical and chemical environmental conditions samples were taken by ROV QUEST 5 whenever possible, in order to enable precise location and characterisation of the sampling site and the sample properties. In addition water and sediment samples were taken by a CTD-rosette sampler and a TV-grab. Samples were processed immediately and in addition stored to be used in the home lab.

- The most important sampling devices during this cruise were those adapted to and managed by the ROV. These made it possible to take samples from exactly defined and recognised local sites.
  - Water samples taken by 5l-Niskin bottles mounted to the drawer of the ROV were filtered (polycarbonate membrane filters, pore size 0.2  $\mu\text{m}$ ) and stored at 4°C for cultivation, frozen at -20°C or stored at -20°C in glycerol. Material from these samples also was used for enrichment cultures.
  - At selected sites, microorganisms from hydrothermal fluids were collected by in-situ filtration (up to 60 liter) on membrane filters (polycarbonate membrane filters, pore size 0.2  $\mu\text{m}$ ) using a pump connected to the fluid sampling system or in bottles of the fluid sampling system used by the geochemical. Filter material was used for enrichment cultures or stored at 4°C, frozen at -20°C or stored at -20°C in glycerol.
  - Rock samples taken by the manipulator arm were immediately used for enrichment cultures or stored at 4°C and frozen at -20°C.

- Sediment samples from 6 stations with the TV-grab, including hot sediments with large numbers of mussels, were used for enrichment cultures and also stored at -20°C for genetic analysis in the home lab.
- Water samples from 17 depth profiles at various sites within the Logatchev-field were taken with Niskin bottles (CTD-rosette sampler). Microorganisms were concentrated on filters and stored at -20°C.

With selected samples enrichment cultures and serial dilution series were inoculated immediately after sampling. A variety of media was used to cultivate bacteria involved in sulfur oxidation either aerobically or anaerobically. For isolation of aerobic bacteria suitable samples were diluted and plated on agar plates for separation and isolation. Temperature gradients were created in a heated and cooled metal block from 20 to 80°C and experiments set up to characterise the response of bacterial communities in regard to the selected temperature range.

#### **3.4.11.4 Preliminary results**

In contrast to our expectations the hydrothermal fluid samples obtained from locations inside the Logatchev field contained very low amounts of reduced sulfur compounds (see chemistry section). This result was confirmed by a low abundance of chemolithoautotrophic and mixotrophic sulfur-oxidizing bacteria as indicated by incubation experiments conducted in specific media during the cruise.

#### **3.4.12 Weather conditions during M60/3**

(Torsten Truscheit)

When R/V METEOR left the port of Fort-de-France/Martinique on the evening of the 16<sup>th</sup> January, northeastern winds of Bft 3 prevailed with the sky partly overcast and showers of rain. On the way to the working area 1, the “Logatchev Hydrothermal Field” on 14°45’N/44°59’W it was mainly cloudy with light to moderate showers of rain. The wind increased up to Bft 4 to 5, coming constantly from the east.

A low 948 hPa over Newfoundland on the 17<sup>th</sup> of January moved northeastwards, its swell reaching the working area with some temporal delay causing a delay of the dive of the ROV QUEST planned for the 21<sup>st</sup> of January. The swell reached a height of up to 4 meters coming from the north. An additional swell coming from easterly directions made the working with the ROV QUEST even more difficult.

Simultaneously a high southwest of the Canary Islands respectively north of the Cape Verde Islands remained stationary over a long period. Another high build up at the 30<sup>th</sup> of January east of Florida and moved further eastward connecting with the above mentioned high from which a wedge of 1018 hPa extended to the working area up to the 3<sup>rd</sup> February.

During the whole period repeatedly new lows built up over or closely east of New Foundland, initially moving eastward, veering northeastwards south of Cape Farvel. Therefore, a more or less significant swell with a relatively long period up to 14 seconds from northnorthwest

remained. Together with a second swell coming from easterly directions this made working conditions difficult until the end of the cruise.

During the whole period the trade wind blew with Bft 4 to 5 with rare and only insignificant exceptions.

Beginning on the 6<sup>th</sup> of February the wind started to increase up to Bft 6 to 7 with gusts Bft 8 (40 kts) causing seas up to 4,5 meters, so that further dives of the ROV QUEST had to be cancelled.

There was no significant change of weather conditions during the transit back to Fort-de-France. R/V METEOR arrived at Fort-de-France/Martinique on the 13<sup>th</sup> of February.

- References**
- Aldrich, A.P. and van den Berg, C.M.G. (1998). Determination of iron and its redox speciation in seawater using catalytic stripping voltammetry. *Electroanalysis* 10: 369-373.
- Application Bulletin Metrohm 123/3 – Voltammetric determination of iron and manganese
- Application Bulletin Metrohm 226/2 – Determination of arsenic by anodic stripping voltammetry at the rotating gold electrode.
- Application Bulletin Metrohm 231/2 – Voltammetric determination of zinc, cadmium, lead, copper, thallium, nickel, and cobalt in water samples according to DIN 38406
- Barra, C.M. and dos Santos, M.M.C. (2001). Speciation of inorganic arsenic in natural waters by square wave cathodic stripping voltammetry. *Electroanalysis* 13: 1098-1104.
- Batuyev, B.N., Kratov, A.G., V.F., M., G.A., C., S.G., K. and Y.D., L., 1994. Massive sulfide deposits discovered at 14°45'N Mid-Atlantic Ridge. *Bridge Newsletter* 6: 6-10.
- Boussemart, M., van den Berg, C.M.G., and Ghaddaf, M. (1992). The determination of the chromium speciation in sea water using catalytic cathodic stripping voltammetry. *Anal. Chim. Acta* 262: 103-115.
- Campbell, B.J., Jeanson, C., Kostka, J.E., Luther III, G.W., and Cary, S.C. (2001) Growth and phylogenetic properties of novel bacteria belonging to the epsilon subdivision of the proteobacteria enriched from *Alvinella pompejana* and deep-sea hydrothermal vents. *Appl. Environ. Microbiol.*: 67, 4566-4572.
- Charlou, J.-L. and Donval, J.-P., 1993. Hydrothermal Methane Venting Between 12°N and 26°N Along the Mid-Atlantic Ridge. *J. Geophys. Res.* 98(B6): 9625-9642.
- Charlou, J. L., Donval, J. P., Fouquet, Y., Jean-Baptiste, P., and Holm, N. (2002). Geochemistry of high H<sub>2</sub> and CH<sub>4</sub> vent fluids issuing from ultramafic rocks at the Rainbow hydrothermal field (36°14'N, MAR). *Chem. Geol.* 191: 345-359.
- Cherkashev, G.A., Ashadze, A.M., and Gebruk, A.V., 2000. New fields with manifestations of hydrothermal activity in the Logatchev area (14°N, Mid-Atlantic Ridge). *InterRidge News* 9(2): 26-27.
- Cline, J. D. (1969). Spectrophotometric determination of hydrogen sulfide in natural waters. *Limnol Oceanogr* 14: 454-458.
- Corre, E., Reysenbach, A.L., and Prieur, D. (2001) ε-Proteobacterial diversity from a deep-sea hydrothermal vent on the Mid-Atlantic Ridge. *FEMS Microbiol. Lett.*: 205, 329-335.
- Douville, E., Charlou, J.L., Oelkers, E.H., Bienvenu, P., Jove Colon, C.F., Donval, J.P., Fouquet, Y., Prieur, D., and Appriou, P. (2002). The rainbow vent fluids (36°14'N, MAR): the influence of ultramafic rocks and phase separation on trace metal content in Mid-Atlantic Ridge hydrothermal fluids. *Chem. Geol.* 184: 37-48.

- Eberhardt, G.L., Rona, P.A., and Honnorez, J., 1988. Geologic Controls of Hydrothermal Activity in the Mid-Atlantic Ridge Rift valley: Tectonics and Volcanism. *Mar. Geophys. Res.* 10: 233-259.
- Gebruk, A.V., Chevaldonné, P., Shank, T., Lutz, R.A., and Vrijenhoek, R.C., 2000. Deep-sea hydrothermal vent communities of the Logatchev area (14°45'N, Mid-Atlantic Ridge): diverse biotopes and high biomass. *J. Mar. Biol. Assoc. U. K.*, 80: 383-393.
- German, C.R. and Parson, L.M., 1998. Distributions of hydrothermal activity along the Mid-Atlantic Ridge: interplay of magmatic and tectonic controls. *Earth Planet. Sci. Lett.* 160: 327-341.
- Grasshoff, K. (1983). Determination of oxygen. In *Methods of Seawater Analysis* (ed. K. Grasshoff, M. Ehrhardt, and K. Kremling), pp. 61-72. Verlag Chemie.
- Jeroschewski, P., Steukart, C., and Kühl, M. (1996). An amperometric microsensor for the determination of H<sub>2</sub>S in aquatic environments. *Anal. Chem.* 68: 4351-4357.
- Kadko, D. C., Rosenberg, N. D., Lupton, J. E., Collier, R. W., and Lilley, M. D. (1990). Chemical reaction rates and entrainment within the Endeavour Ridge hydrothermal plume. *Earth Planet. Sci. Lett.* 99: 315-335.
- Kühl, M., Steukart, C., Eickert, G., and Jeroschewski, P. (1998). A H<sub>2</sub>S microsensor for profiling biofilms and sediments: application in an acidic lake sediment. *Aq. Microb. Ecol.* 15: 201-209.
- Luther III, G.W., Giblin, A.E., and Varsolona R. (1985). Polarographic analysis of sulfur species in marine porewaters. *Limnol. Oceanogr.* 30: 727-736
- Madureira, M.J., Vale, C., and Simões Gonçalves, M.L. (1997). Effect of plants on sulphur geochemistry in the Tagus salt-marshes sediments. *Mar. Chem.* 58: 27-37.
- Mozgova, N.N., Efimov, A.V., Borodaev, Y.S., Krasnov, S., Cherkasov, G.A., Stepanova, T.V., and Ashadze, A.M., 1999. Mineralogy and Chemistry of Massive Sulfides from the Logatchev Hydrothermal Field (14°45'N Mid-Atlantic Ridge). *Exploration Min. Geol.* 8(3): 379-395.
- Pfender, M. and Villinger, H. (2002). Miniaturized data loggers for deep sea sediment temperature gradient measurements. *Mar. Geol.* 186: 557-570.
- Revsbech, N. P. & Jørgensen, B. B. (1986). Microelectrodes and their use in microbial ecology. In *Advances in Microbial Ecology*, Vol. 9 (ed. K. C. Marshall), pp. 293-352. Plenum Press.
- Revsbech, N. P. (1989). An oxygen microelectrode with a guard cathode. *Limnol. Oceanogr.* 34: 474-478.
- Reysenbach, AL, Longnecker, K., and Kirshtein, J. (2000) Novel bacterial and archaeal lineages from an in situ growth chamber deployed at a Mid-Atlantic ridge hydrothermal vent. *Appl. Environ. Microbiol.*: 66, 3798-3806.
- Rona, P.A., Bougalt, H., Charlou, J.L., Appriou, P., Nelsen, T.A., Trefry, J.H., Eberhart, G.L., Barone, A., and Needham, H.D., 1992. Hydrothermal circulation, serpentinization, and degassing at a rift valley-fracture zone intersection: Mid-Atlantic Ridge near 15°N, 45°W. *Geology* 20: 783-786.
- Sander, S. and Koschinsky, A. (2000). Onboard-ship redox speciation of chromium in diffuse hydrothermal fluids from the North Fiji Basin. *Mar. Chem.* 71: 83-102.

- Seifert, R., Dellinger, N., Richnow, H.H., Kempe, S., Hefter, J., and Michaelis, W. (1999). Ethylene and methane in the upper water column of the subtropical Atlantic. *Biogeochemistry* 44: 73-91.
- Sudidarikov, S. and Zhirnov, E. (2001). Hydrothermal plumes along the Mid-Atlantic-Ridge: preliminary results of CTD investigations during the DIVERS Expedition (July 2001). *InterRidge News*, 10(2): 33-36.
- Teske, A., Brinkhoff, T., Muyzer, G., Moser, D.P., Rethmeier, J., and Jannasch, H.W. (2000). Diversity of thiosulfate-oxidizing bacteria from marine sediments and hydrothermal vents. *Appl. Environ. Microbiol.*: 66, 3125-3133.
- van den Berg, C.M.G. and Khan, S.H. (1990). Determination of selenium in sea water by adsorptive cathodic stripping voltammetry. *Anal. Chim. Acta* 231: 221-229